



Insight on bacteria communities in outdoor bronze and marble artefacts in a changing environment



Andrea Timoncini ^a, Federica Costantini ^{b,c,d}, Elena Bernardi ^e, Carla Martini ^f, Francesco Mugnai ^b, Francesco Paolo Mancuso ^g, Enrico Sassoni ^h, Francesca Ospitali ^e, Cristina Chiavari ^{a,*}

^a Department of Cultural Heritage, University of Bologna, Via degli Ariani 1, 48121 Ravenna, Italy

^b Department of Biological, Geological and Environmental Science, UOS Ravenna, University of Bologna, Via Sant'Alberto 163, 48123 Ravenna, Italy

^c Interdepartmental Center for Industrial Research Renewable Sources, Environment, Sea and Energy, University of Bologna, Ravenna, Italy

^d Interdepartmental Research Center for Environmental Sciences, University of Bologna, Ravenna, Italy

^e Department of Industrial Chemistry "Toso Montanari", University of Bologna, Viale del Risorgimento 4, 40136 Bologna, Italy

^f Department of Industrial Engineering, University of Bologna, Viale del Risorgimento 4, 40136 Bologna, Italy

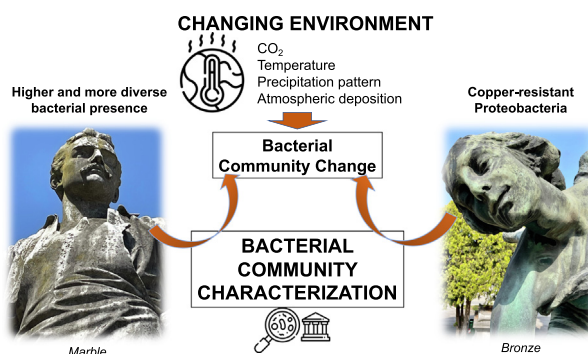
^g Department of Earth and Marine Sciences (DiSTeM), University of Palermo, Viale delle Scienze Ed. 16, 90128 Palermo, Italy

^h Department Of Civil, Chemical, Environmental and Materials Engineering, University of Bologna, Via Terracini 28, 40131 Bologna, Italy

HIGHLIGHTS

- Chemical composition of bronze and marble patinas in outdoor environment
- Significant difference in bacterial communities between marble and bronze statues
- Sheltered bronze areas show the strongest bacteria inhibition due to Cu.
- On marble, Cu and Ca oxalate are present where Cu ions percolation occurs.
- Typical bacteria communities on bronze and marble patinas were identified.

GRAPHICAL ABSTRACT



ARTICLE INFO

Editor: Ewa Korzeniewska

Keywords:

Climate change
High throughput sequencing
Cultural heritage
Corrosion
Copper alloys
Biodegradation

ABSTRACT

Epilithic bacteria play a fundamental role in the conservation of cultural heritage (CH) materials. On stones, bacterial communities cause both degradation and bioprotection actions. Bronze biocorrosion in non-burial conditions is rarely studied. Only few studies have examined the relationship between bacteria communities and the chemical composition of patinas (surface degradation layers). A better comprehension of bacterial communities growing on our CH is fundamental not only to understand the related decay mechanisms but also to foresee possible shifts in their composition due to climate change. The present study aims at (1) characterizing bacterial communities on bronze and marble statues; (2) evaluating the differences in bacterial communities' composition and abundance occurring between different patina types on different statues; and (3) providing indications about a representative bacterial community which can be used in laboratory tests to better understand their influence on artefact decay. Chemical and biological characterization of different patinas were carried out by sampling bronze and marble statues in Bologna and Ravenna (Italy), using EDS/Raman spectroscopy and MinION-based 16SrRNA sequencing. Significant statistical differences were found in bacterial composition between marble and bronze statues, and among marble patinas in different statues and in the same statue. Marble surfaces showed high microbial diversity and were characterized mainly by Cyanobacteria, Proteobacteria and Deinococcus-Thermus. Bronze patinas showed low taxa

* Corresponding author.

E-mail address: cristina.chiavari@unibo.it (C. Chiavari).



diversity and were dominated by copper-resistant Proteobacteria. The copper biocidal effect is evident in greenish marble areas affected by the leaching of copper salts, where the bacterial community is absent. Here, Ca and Cu oxalates are present because of the biological reaction of living organisms to Cu ions, leading to metabolic product secretions, such as oxalic acid. Therefore, a better knowledge on the interaction between bacteria communities and patinas has been achieved.

1. Introduction

The conservation of outdoor cultural heritage (CH) materials (i.e., bronze and marble) is significantly influenced by both abiotic and biotic factors. Abiotic factors include pollutants and atmospheric depositions (Spezzano, 2021; Tidblad et al., 2016; Watt et al., 2009) and all climatic and meteorological parameters (Brimblecombe, 2003; Sabbioni et al., 2010; Spezzano, 2021), such as fluctuation of temperature (Kong et al., 2016; Liu et al., 2015; Samie et al., 2007; Toreno et al., 2018), sunlight exposure and intensity, wind, relative humidity (Liu et al., 2015) and wetting time (Cole et al., 2007). Biotic factors include all living organisms (e.g., bacteria, fungi, lichens) growing on cultural heritage materials.

The interaction between abiotic and biotic factors (Toreno et al., 2018; Vidal et al., 2019) leads to the formation of characteristic layered degradation products on the material surface, the so-called “patina” (Scheerer et al., 2009). This patina could have protective or not protective properties towards the original surface, depending on its chemical and biological composition and physical characteristics. Concerning stones, the ICOMS glossary defined the term “patina” as: “chromatic modification of the material, generally resulting from natural or artificial ageing and not involving in most cases visible surface deterioration” (Vergès-Belmin et al., 2008). For sake of clarity, in this paper, both for stones and metals, we call “patina” any surface modification of the original substrate.

1.1. Patinas on bronze

Concerning outdoor bronze artefacts, the patina generally shows a two-layer structure depending on the exposition to the rain. Indeed, patinas not exposed to runoff, show the inner layer constituted by Cu I and Sn IV oxides with enrichment in Sn products and chlorides, while the external layer is mainly composed of Cu II salts, oxides, chlorides and sulfates of Cu and Pb (Chiavari et al., 2010). The wide range of patina colours (e.g., pale green, black and dark green) and the chemical composition have been extensively investigated and related to atmospheric composition as well as to the action of rain and microclimatic conditions (Bernard and Joiret, 2009; Bernardi et al., 2009; Brimblecombe, 2003; Cao and Xu, 2006; Chiavari et al., 2010, 2015; Graedel et al., 1987; Nassau et al., 1987). Picciochi et al. (2004) reported the formation, on bronze, of different compounds depending on urban or marine atmospheres. The former induces the formation of cuprite (Cu_2O), brochantite ($\text{Cu}_4\text{SO}_4(\text{OH})_6$), posnjakite ($\text{Cu}_4(\text{SO}_4)(\text{OH})_6(\text{H}_2\text{O})$), atacamite ($\text{Cu}_2\text{Cl}(\text{OH})_3$) and paratacamite ($\text{Cu}_3(\text{Cu}, \text{Zn})(\text{OH})_6\text{Cl}_2$), while the marine atmosphere promotes only cuprite, atacamite and paratacamite.

The origins of brochantite and posnjakite could be ascribed to the sulfur compounds coming mainly from atmospheric deposition, while atacamite and paratacamite occur as a chloride corrosion product on bronze artefacts (de Oliveira et al., 2009; Picciochi et al., 2004).

Specifically, in outdoor quaternary bronze statues, the areas exposed to rainfall are characterized by a pale green patina. This patina consists of two-layer structures: the external layer is relatively enriched in Sn by comparison to Cu, Pb and Zn, with a high concentration of atmospheric elements; the inner layer is brown and compact and characterized by a lower concentration of atmospheric elements and higher Cu concentration than the external one (Chiavari et al., 2007).

1.2. Patinas on marble

Concerning outdoor marble artefacts, patina formation is mostly influenced by how rainwater wets the surface. Two areas may be distinguished clearly, white and black. The former is exposed to water runoff and appears white due to cyclic washing out of deposits and deterioration products eventually formed; it is mainly composed of calcium carbonate, with the possible presence of magnesium carbonate (in the case of dolomitic marbles) (Brimblecombe, 2003; Camuffo et al., 1982). Conversely, black areas form on surfaces protected from direct rain runoff. This condition favours the sulfation of the surface, with the formation of a crust mainly composed of gypsum and able to trap black carbonaceous and metal atmospheric particles (Camuffo et al., 1982). An important type of marble patina is the one composed of oxalate, specifically, Ca-oxalate, known for its material consolidating capacity, and very common among calcareous stone surfaces. Indeed, on marble, it can form a uniform and thick layer composed of mainly both whewellite ($\text{CaC}_2\text{O}_4\cdot\text{H}_2\text{O}$) and weddellite ($\text{CaC}_2\text{O}_4\cdot 2\text{H}_2\text{O}$) (Monte, 2003; Perez-Rodriguez et al., 2011). It originates from both atmospheric deposition and biological activity, especially by fungi (Gadd et al., 2014).

1.3. Role of biotic factors: biodegradation and bioprotection

Microbial ecology applied to cultural heritage material is getting increasing attention since several studies have pointed out that the activity of bacteria is responsible not only for degradation and soiling but also for the protection of CH materials (Joseph, 2021; Scheerer et al., 2009; Viles and Cutler, 2012). Until now, most of the research has focused on biological communities on stone, while evidence from bronze artefacts is scarce (Cutler and Viles, 2010; Lamenti et al., 2019; Scheerer et al., 2009; Warscheid and Braams, 2000). In the case of bronze, to our knowledge, only few studies have been performed, preferentially related to buried artefacts (Ghiara et al., 2019; Piccardo et al., 2013), or to biopatination methods for improving conservation (Joseph, 2021) or to antimicrobial effects of copper and copper alloys (Chang et al., 2021a, 2021b).

1.3.1. Biodegradation

In the case of metals, microorganisms' colonization may favour corrosion when anodic or cathodic reactions, or even both, are accelerated. Acidic metabolites can promote both cathodic and anodic reactions, by providing H^+ subsequently reduced at the cathode and enhancing metal dissolution at the anode. Moreover, the acceleration of corrosion may be due also to a decrease in pH with the consequent higher solubility of corrosion products (Videla and Herrera, 2009). Specifically, in anaerobic or waterlogged burial environments, the presence of microorganisms, such as sulfate-reducing bacteria is associated with corrosion via the copper sulfide formation, which in turn may be oxidized to brochantite (Muros and Scott, 2018).

In the case of stones, it has been estimated that bacteria, together with fungi and plants (Scheerer et al., 2009) are responsible for 20–30% of deterioration (Wakefield and Jones, 1998). Biodeterioration can occur through several mechanisms, described in detail in the following, namely biofilm formation, discolouration, metal oxidation/reduction, salting and physical damage, and corrosion induced by inorganic and organic acids (Scheerer et al., 2009).

Biofilm formation. The biofilm originates from microbial cells bounded within the extracellular polymeric substances (EPS), which generally include polysaccharides, pigments, proteins, glycoproteins, lipopolysaccharides, lipids, glycolipids, fatty acids and enzymes (Prieto et al., 2020; Toreno et al., 2018). Their main role is to alter the water transport and retention by changing the capillary water transport, vapour diffusion and wettability, due to the capacity of EPS to act as a buffer for the cells thus decreasing or delaying water evaporation (Schröer et al., 2022). This results in increased cell resistance to drought periods. However, these wetting and drying cycles, with consequent expansion and contraction, weaken the mineral lattice and enhance the dirty appearance of the substrate (i.e., soiling and pigments accumulation) (Viles and Cutler, 2012).

Discolouration. The discolouration is the result of pigments contained within or released by the microorganisms (mainly cyanobacteria) living in the biofilm, such as photosynthetic pigments like chlorophyll, carotenes and melanin, and atmospheric particles trapped in EPS (Gaylarde, 2020; Dias et al., 2020; Viles and Cutler, 2012). Different levels of pigmentation are determined by environmental factors such as light intensity and wavelength, nutrient availability, and temperature. Indeed, cyanobacteria contribute to both yellow-brown colour patina (Macedo et al., 2009) and to the more common black areas in subtropical and tropical areas (Ortega-Morales et al., 2019; Scheerer et al., 2009). Discolouration induces both aesthetic and structural problems since it changes the appearance of the substrate and colour changes and thus also influencing sunlight absorption. This leads to an increase in mechanical stress related to heating/cooling and wetting/drying cycles (Scheerer et al., 2009). Physical damage due to water uptake and increasing pressure within fissures is also due to the penetration of microorganisms, such as cyanobacteria, into the stone (Scheerer et al., 2009).

Metal oxidation/reduction. Stones are subjected to oxidation/reduction of metals present in them. In non-burial conditions, oxidation prevails. The oxidation with the migration of oxidized metals is responsible for discolouration and surface alteration stimulating the patina formation. The role of these patinas can be either protective or degradative as it changes the water retention thus weakening the inner stone (Schröer et al., 2021). Specifically, in marble, bacteria can oxidize lots of metals, in particular, Fe, Mn and Pb. Indeed, on marble bacteria capable to oxidize iron (Bams and Dewaele, 2007) and lead (Cantisani et al., 2019) were detected. The lead oxidation on marble is responsible for red discolouration for the minium (PbO₄) formation (Schröer et al., 2021).

Salting and physical damage. The involvement of bacteria in the salting process, due to the excretion of acids reacting with the stone, is responsible for subsequent physical damages, such as blistering, flaking, cracking, scaling, and granular disintegration. The salting process is also responsible for the increase in the production of EPS and biofilm density with associated degradative consequences as reported by Scheerer et al. (2009).

Corrosion. An important biodeterioration mechanism to which also bacteria contribute is solubilisation via secretion of inorganic or organic acids originated by metabolic processes (Scheerer et al., 2009). The most common inorganic acids found on stone materials are carbonic, sulfurous, sulfuric, nitrous and nitric acids. These acidifying compounds react with the stone forming water-soluble products and leading to its dissolution (Sand et al., 2003; Scheerer et al., 2009). Carbonic acid is responsible for the degradation of calcareous stones, by the so-called karst effect (Lipfert, 1989). The most common organic acids are oxalic, citric, acetic, gluconic, malic, succinic acid, amino acids, nucleic acids and uronic acids. They contribute to stone solubilisation via both salt formation and complexation (Scheerer et al., 2009). Polyfunctional organic acids may show both solubilisation and consolidation action in relation to the substrate chemical composition. For instance, oxalic acid enhances the dissolution of siliceous rocks, while on calcareous stones it leads to calcium oxalate formation, resulting in a protective action (Andreolli et al., 2020; Daskalakis et al., 2013; Salinas-

Nolasco et al., 2004; Scheerer et al., 2009). Finally, bacteria increase their organic acid production during high-stress conditions (Scheerer et al., 2009).

1.3.2. Bioprotection

On metals, microorganisms can exert a protective action because of the consumption of oxygen through aerobic respiration, formation of EPS protective layers or biocompetition between corrosive and non-corrosive species (Albini et al., 2017; Joseph, 2021; Joseph et al., 2012; Videla and Herrera, 2009; Kip and van Veen, 2015).

On stones, bacteria metabolism products, such as EPS, may cause consolidation of the substrate (Daskalakis et al., 2013; Joseph, 2021; Ortega-Villamagua et al., 2020; Scheerer et al., 2009). It is the consequence of mineral precipitation. Indeed, they can produce a wide variety of minerals, including silicates, phosphates, sulfides, oxides, and above all carbonates, since they are common biominerals produced by many bacteria inhabiting stone communities (Boquet et al., 1973). The precipitation process takes place thanks to favourable conditions of pH, calcium concentration, dissolved inorganic carbon concentration and the availability of nucleation sites. Indeed, the increase in alkalinity and the use of their cells as nucleation sites are two common ways to promote mineral precipitation (Hammes and Verstraete, 2002; Schröer et al., 2021; Stocks-Fischer et al., 1999). It is notable to mention that the CaCO₃ precipitation may be mostly stimulated, also for bioconsolidation, via promoting photosynthesis, urea hydrolysis, sulfate reduction, and degradation of amino acids, as reported in (Schröer et al., 2021) and in (Baumgartner et al., 2006; Dupraz et al., 2009; Erşan et al., 2015; Hammes et al., 2003; Rodríguez-Navarro et al., 2003). Specifically, Daskalakis et al. (2013) found that *Pseudomonas*, *Pantoea* and *Cupriavidus* have a biomineralization ability by inducing calcium carbonate precipitation.

1.4. Influence of climatic factors and future climate change on biotic factors

The growth of bacterial communities is influenced by climatic conditions, bioreceptivity and nutrition (Guillitte, 1995; Scheerer et al., 2009; Viles and Cutler, 2012). Specifically, Gladis-Schmacka et al. (2014) stated that the occurrence of biofilms on outdoor materials is mostly determined by climatic conditions, especially humidity, so macroclimate seems to be more important than the material substrate. The nutrient supply comes from the substrate as well as from atmospheric depositions to which pollutants contribute significantly (Zanardini et al., 2000). In fact, SO₂ and N-compounds stimulate, respectively, the growth of sulfur-oxidizing (e.g., *Thiobacillus* spp.) and nitrifying (e.g., *Nitrosomonas* spp. and *Nitrobacter* spp.) bacteria with the production of sulfuric and nitric acid (Dakal and Cameotra, 2012), accelerating the corrosion and dissolution of the underlying material.

In this multi-parameter context, the changes taking place in the climate and in the atmospheric composition (Monks et al., 2009; Pachauri et al., 2014; Spezzano, 2021) must also be considered. Indeed, climate and air quality are closely connected (Monks et al., 2009; Seinfeld and Pandis, 2016; von Schneidmesser et al., 2015). Variations in UV level, water availability, time of wetting, frequency of extreme events and, as already mentioned, the nutrient supply affect the structure and function of the microbial biota living on CH surfaces. This, in turn, leads to biological community structure modification, with possible biodeteriogenic or bioprotective effects (Gladis-Schmacka et al., 2014; Ramirez et al., 2010; Viles and Cutler, 2012).

In high-latitude regions, biological activity and biomass accumulation are expected to increase due to the rise in temperature and precipitation. Conversely, in low-latitude regions, a decline in precipitations coupled with temperature increase is expected to reduce biological activity and biomass accumulation (Gómez-Bolea et al., 2012). Besides, CO₂ increase, up to 700–1000 ppm within 2100 in the worst scenarios (Pachauri et al., 2014; Solomon et al., 2007), will foster the growth of phototrophic organisms. These changes will lead to a shift in the community's structure. Cyanobacteria are expected to replace green algae where hotter and drier

conditions will occur, becoming more important in CH materials degradation as reported by Gaylarde (2020), and Prieto et al. (2020). Moreover, CO₂ enrichment and water scarcity will promote colour change of biofilm on stone (Prieto et al., 2004). In addition, some studies (Kemmling et al., 2004; Prieto et al., 2004; Tourney and Ngwenya, 2014) reported an increase in EPS production with water availability decrease, thus the low-latitude regions will experience higher biodegradation through a higher EPS production.

2. Research aim

Understanding the diversity and structure of microbial communities is therefore fundamental in conservation science, allowing us to (1) obtain more complete information on deterioration mechanisms, (2) monitor the conservation state, and (3) understand their possible evolution in the context of climate change.

Nevertheless, until now no studies have assessed the differences in microbial community composition between different areas on the same material exposed outdoors, especially in the case of bronze surfaces.

A wider and deeper knowledge of biological communities on real outdoor artefacts will also allow for the inclusion of representative biological agents, in addition to the chemical and physical ones, in the set-up of accelerated ageing tests, which play a key role both in degradation mechanism studies and in protective treatment assessment.

Based on the above, the present work aims at providing an insight into the composition and structure of bacterial communities living on bronze and marble, through the development of a method that combines the non-invasive sampling requirement typical of CH artefacts, with the rapidity and high identification effectiveness of the metabarcoding sequencing of 16S rDNA gene, via Minion, which is a fast method to characterize the bacterial communities as already shown in (Grottoli et al., 2020).

For this purpose, we: i) characterized bacterial communities on bronze and marble CH surfaces (investigating selected outdoor artefacts); ii) evaluated the influence of the chemical composition of the material substrate on the bacterial community; and iii) provided indications on a representative bacterial community to be included in laboratory ageing tests for simulating the biological effects.

3. Materials and methods

3.1. Study sites and statues

To characterize microbial communities and chemical profiles of different types of patinas, marble and bronze statues were sampled in two cities

Table 1
Sampled Statue's name, material, patina type and location.

Material	Location	Statue	Patina colour
Marble	Bologna	Pompeo Legnani	Black (<i>unsheltered</i>) White (<i>unsheltered</i>) Green basement (<i>unsheltered</i>)
		Gaetano Simoli a.k.a. Fabbro	Black (<i>unsheltered</i>) Black (<i>sheltered</i>) White (<i>unsheltered</i>) Yellow (<i>unsheltered</i>)
	Ravenna	Alfredo Oriani	Pale green (<i>unsheltered</i>) Dark green (<i>sheltered</i>) Black (<i>sheltered</i>) Pale green (<i>unsheltered</i>) Green (<i>unsheltered</i>) Black (<i>sheltered</i>)

in northern Italy (Po Valley): Bologna and Ravenna, the latter being close to the Adriatic Sea. The two locations show comparable air quality and climatic conditions. As summarized in Fig. 1 and Table 1, two marble and one bronze statues were sampled in Bologna (in the Monumental Cemetery of Certosa) and one bronze statue in Ravenna:

- “Pompeo Legnani” (Bologna, 1913), marble
- “Gaetano Simoli” a.k.a. “Fabbro” (Bologna, 1895), marble
- “Trentini Monument” (Bologna, 1924), bronze
- “Alfredo Oriani” (Ravenna, 1899), bronze

3.2. Sampling

For each statue, different types of surface altered layers (patinas) were sampled, as shown in Fig. 2 and Table 1. A distinction was made between “unsheltered” (i.e., directly exposed to rainwater runoff) and “sheltered” areas (i.e., where rainwater runoff does not occur).

The patinas from Pompeo Legnani come from the marble basement of the bronze relief. Specifically, the green patina of “Pompeo Legnani” was chosen to compare marble areas affected by percolation of copper ions leached from the overlying bronze relief with other marble areas not affected by copper percolation. Each patina was chosen since it shows specific colour and degradation pattern: for marble, most of the sample surfaces show discolouration with colours ranging from white to yellow and black, for bronze, the colour varies from black to green to pale green.

To collect bacterial communities growing on each patina, sterile cotton swabs moistened with 100 µL of sterile nuclease-free water were used to rub approximately 25 cm² of the surface. The frame used for the sampling



Fig. 1. Statues sampled in Bologna (the first three) and in Ravenna (the last one), Italy. The number stands for the patina type: “Pompeo Legnani”, 1 = black (*unsheltered*), 2 = green basement (*unsheltered*), 3 = white (*unsheltered*); “Gaetano Simoli” a.k.a. “Fabbro”, 1 = black (*sheltered*), 2 = black (*unsheltered*), 3 = white (*unsheltered*), 4 = yellow (*unsheltered*); “Trentini Monument”, 1 = pale green (*unsheltered*), 2 = black (*sheltered*), 3 = dark green (*sheltered*); (d) “Alfredo Oriani”, 1 = green (*unsheltered*), 2 = pale green (*unsheltered*), 3 = black (*sheltered*).

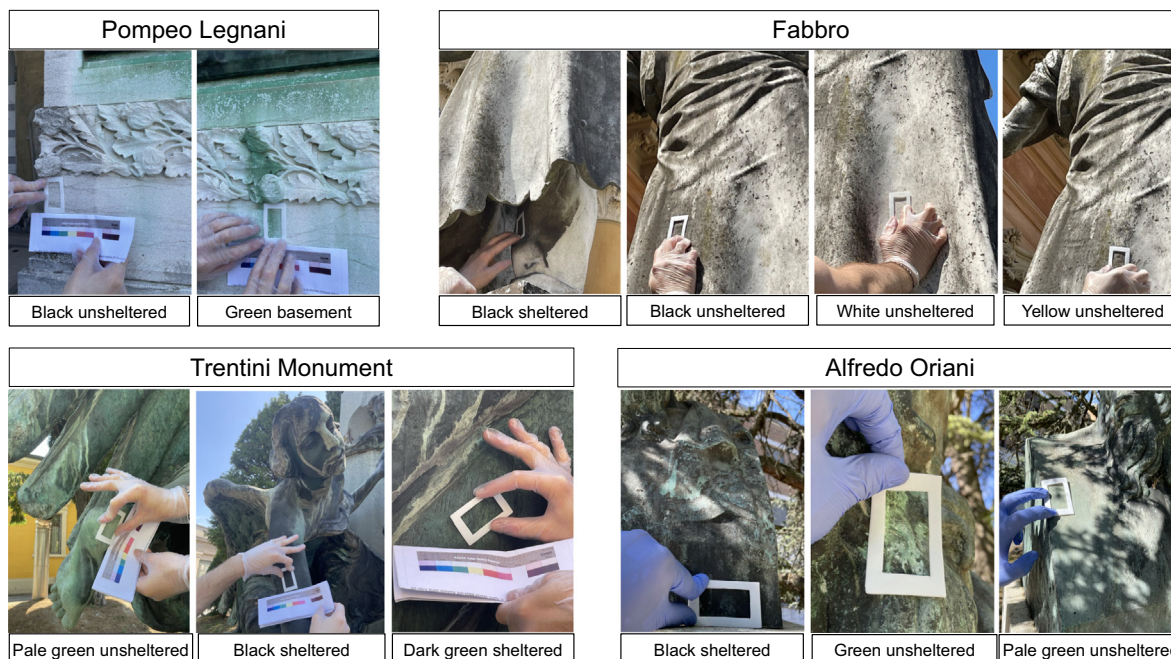


Fig. 2. Examples of patina types sampled, with the frame used for sampling (white rectangle). Above the marble patinas, below the bronze patinas.

is shown in Fig. 2, and it was sterilized with bleach before each sampling. For each statue and patina, two replicates were collected. Swabs were immediately placed in sterile 1.5 mL Eppendorf tubes and stored in dry ice while in the field, then at $-20\text{ }^{\circ}\text{C}$ until DNA extraction. Sampling for chemical-mineralogical characterization of the patinas was performed using a chisel.

3.3. Chemical-mineralogical characterization of the patinas

Mineralogical characterization of the sampled patinas was performed by Raman micro-spectroscopy (Renishaw Raman Invia Spectrometer configured with a Leica DMLM microscope). The exciting source was an Ar^{+} ion laser (514.5 nm), with settings optimised to avoid sample degradation and obtain a satisfying S/N ratio (laser power $P_{\text{out}} = 1.5\text{ mW}$, accumulation time $t = 10\text{ s}$, number of scans $n = 4$), despite the high fluorescence. For this reason, a baseline subtraction was necessary, carried out by Renishaw WiRE2.0 software.

Raman identifications were done by comparison with spectra of pure standards contained in the online RRUFF Project Raman spectra database (Database of Raman Spectroscopy, X-ray Diffraction and Chemistry of Minerals) and/or with the cited bibliography.

Chemical composition was analyzed by scanning electron microscopy (SEM, Zeiss EP EVO 50) equipped with an Energy Dispersive Spectroscopy (EDS) microprobe (Oxford Instruments INCA X-act Penta FET® Precision [$z > 4$ (Be), resolution 129 eV (MnKa @ 2500cps)]) with INCA Microanalysis Suite Software (version 4.15- issue.18 service pack 5). The analyses on patina powders were carried out at EHT 20 keV in High Vacuum ($\sim 10^{-4}$ Pa) conditions.

3.4. Biological characterization of the bacterial communities

Microbial DNA was extracted using the E.Z.N.A.® SOIL DNA KiT (Omega Bio-Tek) inserting the cotton swab inside the first tube provided by the manufacturer. Similar kits, (e.g., Fast DNA SPIN Kit for Soil (MP Bio-medicals, Illkirch, France)) were already used to extract the DNA from different sources, such as marble, stone, and metal (Piñar et al., 2019; Sanmartín et al., 2015). DNA extractions from negative controls based on laboratory aerosol (Eppendorf opened on the workbench during the extraction procedure) were conducted at the end of each extraction following the

same procedure as the real samples. DNA yield was assessed using the Qubit dsDNA HS Assay Kit with a Qubit 2.0 fluorometer (Invitrogen).

16S sequencing libraries were generated using the 16S Barcoding Kit (SQK-16S024) from Oxford Nanopore Technologies (ONT), Oxford, UK, following the manufacturer's instructions. 10 ng of DNA were employed for PCR amplification, where 30 PCR cycles were chosen instead of 25 to increase reaction yield. The entire PCR process was composed of initial denaturation at $95\text{ }^{\circ}\text{C}$ for 1 min, denaturation at $95\text{ }^{\circ}\text{C}$, annealing at $55\text{ }^{\circ}\text{C}$ and extension at $65\text{ }^{\circ}\text{C}$ for 30 cycles, followed by a final extension at $65\text{ }^{\circ}\text{C}$ for 1 min. Negative PCR controls were also included for each batch of PCRs. Targeted samples were pooled in equimolar ratios and about 82 fmol of the pooled sample were loaded onto a MinION flow cell (R10.3, FLO-MIN111). The flow cell was placed into the MinION for the sequencing and controlled using ONT's MinKNOW 4.3.12 (Oxford Nanopore Technologies, Oxford, UK) software. The Nanopore technology was chosen since it is getting frequently used in CH conservation (Pavlovic et al., 2021), especially for the characterization of microbial communities on walls and stone (Adamiak et al., 2018a, 2018b; Grottole et al., 2020; Piñar et al., 2020a) and painting (Piñar et al., 2020b).

It allows to immediately sequence directly in the laboratory for real-time analysis (Grottole et al., 2020; Magi et al., 2017; Nygaard et al., 2020; Piñar et al., 2019, 2020a) of the long-reads 16S rRNA amplicon V3 and V4 hypervariable regions of the 16S rRNA gene (Pyzik et al., 2021). The use of long-reads 16S rRNA amplicon in Nanopore MinION brings the accuracy in taxa identification to $\sim 95\%$ (Santos et al., 2020).

The base-called data (fastq) were further processed using the 16S-workflow available in the cloud-based data analysis platform EPI2ME (Piñar et al., 2020a) with "Fastq 16S Analysis" and the average quality of about 85 %, for demultiplexing. The reads were clustered at MOTU (Molecular Operational Taxonomic Unit) level (based on EPI2ME, here output MOTUs are ranked at the species level).

The relative abundance of each species within each sample was calculated, and the species were sorted in descending order by relative abundance retaining only the species with a relative abundance higher than 0.1 %. The relative species abundance of the two replicates per patina and statue was averaged to get the abundances per patina type. The species abundance per material was obtained by averaging the species abundance of each patina of the same material. For graphical representation, the species were then collapsed to phylum and genus levels since the first

represents the biggest group below the superkingdom of bacteria, while the genus level comes above species. For statistical analysis, we worked at the species level (see below). The species abundance table and the associated taxonomic table are available under request.

3.5. Data analysis

To estimate alpha diversity, the species abundance table was rarefied at the number of sequences of the sample with the least sequencing depth (n . reads = 1690, “Fabbro” sheltered replicate 2). Data were rarefied using the “rarefy_even_depth” function in the “Phyloseq” library (we defined a random number of seeds to 15, R environment) (McMurdie and Holmes, 2013) 2177 MOTUs were removed because they are no longer present in any sample after random subsampling.

Alpha diversity was assessed for both materials (bronze and marble) and patina types. The following diversity indices were calculated on rarefied untransformed data: total taxa richness (S), Margalef's index (d), Shannon's index (H') and Pielou's index (J). The Margalef index (Margalef, 1958) estimates the total number of species but incorporates also the total number of individuals (N) to adjust for the fact that within a larger number of individuals, more species may expect to be found, the Shannon index takes into account for both richness and evenness, while Pielou's (Pielou, 1966) estimates the species evenness. We calculated mean values and standard errors for each of these metrics for each material and patina type.

Differences in alpha diversity indexes and microbial community structure between Materials (fixed factor, 2 levels: marble and bronze) and Patina (fixed factor, 7 levels, nested within Materials) were statistically tested by performing univariate and multivariate permutational analyses of variance (PERMANOVA) with PERMANOVA+ (Anderson Marti et al., 2008) in PRIMER v.7 (Clarke and Gorley, 2015). To perform PERMANOVAs, we created euclidean distance matrixes on untransformed data for each alpha diversity index; while for multivariate analysis a Bray-Curtis similarity matrix on the fourth-root transformed abundance data were made. Due to the unbalanced sampling design, we used type III sum of squares and unrestricted permutation of the raw data with 9999 permutations. When the factor Patina was found to be statistically significantly different, a pairwise a posteriori comparison was performed using the Permutation test of Monte Carlo due to the low number of possible permutations.

Variability in the bacterial community structure among samples was displayed by unconstrained ordination plots using the principal coordinate analysis (PCO), based on Bray-Curtis distance matrix calculated from the fourth-root transformed MOTU abundance data.

All the analyses were performed using R statistical software (Version 4.1.1) (R Core Team, 2021) unless otherwise specified.

4. Results

4.1. Chemical-mineralogical characterization of the patinas

Results of EDS analyses of the bronze patinas on the “Trentini monument” and “Alfredo Oriani” are reported in Table 2 (Supplementary material, (SM)), together with those of the marble basement subjected to percolation of soluble corrosion compounds leached from the bronze relief of “Pompeo Legnani”. S, Cl, O, C, Si, Ca and Al are the main environmental elements present in the bronze patinas, with a higher concentration of Cl in the statue located in Ravenna (closer to the sea). Copper concentration in the green part of the marble basement of “Pompeo Legnani” shows a comparable value to those of pale green patinas on bronze (12.4 vs 12.6–13.5 wt%).

The ex-situ Raman analysis reveals the presence of similar mineralogical composition in the same patina type from different statues.

The bronze patinas analyzed are (i) unsheltered pale green (ii) and sheltered black or (iii) sheltered dark green. The results are reported in Fig. 3c and Table 3.

Specifically, concerning bronze patinas, each one shows the presence of copper oxides, carbon, and organic compounds. Besides, as expected, and in agreement with EDS, the unsheltered pale green patina shows mainly the presence of basic sulfate compounds (brochantite, $\text{Cu}_4(\text{SO}_4)(\text{OH})_6$ and antlerite $\text{Cu}_3(\text{SO}_4)(\text{OH})_4$) in both statues. Also, in the “Alfredo Oriani” statue (Ravenna), covellite (CuS) is present together with brochantite. It is worth noting that in the unsheltered pale green patina of “Trentini Monument” (BO) Raman spectrum of carotenoids was found, with intense bands around 1155 cm^{-1} and 1515 cm^{-1} , due respectively to the C—C and C=C stretching of the polyenic chain, and their overtones and combination bands (Schulz et al., 2005). This finding is consistent with biological analysis results. Concerning the sheltered dark green patinas, while the statue in Bologna shows the presence of antlerite, anglesite (PbSO_4) and hydrocerussite ($\text{Pb}_3(\text{CO}_3)_2(\text{OH})$), the statue in Ravenna, much closer to the sea, shows mainly atacamite ($\text{Cu}_2\text{Cl}(\text{OH})_3$), according to the higher concentration of Cl detected by EDS, and only traces of sulphates and cuprite.

From an analytical point of view, the attribution of Raman spectra was performed considering that the mineral brochantite is well defined by the bands at 3400 , 3561 – 3583 cm^{-1} , in the OH^- stretching region, and by the peaks in the lower wavenumber region at 238 , 390 , 450 , 482 , 510 , 590 – 607 – 622 , 973 cm^{-1} (Martens et al., 2003) (Fig. 3). Antlerite shows peaks for both statues at 415 , 478 , 600 , 987 , 1079 , 3489 and 3580 cm^{-1} . Atacamite shows peaks around 125 – 145 , 356 , 840 – 905 – 975 , 3352 – 3440 cm^{-1} (Hayez et al., 2004).

Raman analyses of marble statues (Fig. 3a, b; Table 3) show the common presence of calcite in all patina types, in particular in “unsheltered” samples, together with quartz, anatase, silicates and carbon, which becomes predominant in black areas.

On the sheltered black areas, as expected, gypsum is identified, with the main peak of the SO_4^{2-} stretching at 1008 cm^{-1} , together with weddellite, the hydrate Ca-oxalate, with its characteristic band of the C=O oxalate at 1474 cm^{-1} (Frost, 2004). On marble patinas exposed to the sun, carotenoids are present. Only on the green basement and white area of “Pompeo Legnani” carotenoids are not detected.

Furthermore, on black unsheltered and yellow patinas in the “Fabbro” marble statue, Raman spectroscopy shows the presence of structures similar to phycocyanins (Szalontai et al., 1994), that have the light-harvesting function in cyanobacteria.

The analyses performed on the marble basement (Fig. 3a) of the “Pompeo Legnani”, where greenish stains are present due to the leaching of bronze patina on the marble surface, show the presence of copper salts like brochantite, antlerite (traces) and the Cu-oxalate, moolooite ($\text{Cu}(\text{C}_2\text{O}_4) \cdot 0.4\text{H}_2\text{O}$) (Frost, 2004). Moreover, salts in transformation due to the interaction with calcium carbonate are detected. Specifically, the basic hydrated calcium and copper sulphate, devilline ($\text{CaCu}_4(\text{SO}_4)_2(\text{OH})_6 \cdot 3(\text{H}_2\text{O})$), is found. Devilline is a product formed by the interaction between copper sulphates like brochantite or antlerite and calcite and is characterized by Raman peaks at 412 , 440 , 992 , 1133 , 3560 – 3600 cm^{-1} . A similar process occurs on “Alfredo Oriani” marble basement (not reported in Table 3), where Raman bands at 172 – 195 , 545 , 1456 , 1683 , 3440 – 3470 cm^{-1} could reasonably be ascribed to an intermediate species between pure Ca-oxalates (weddellite or wewhellite) and Cu-oxalate (moolooite).

4.2. Biological characterization of the bacterial communities

4.2.1. DNA extraction

All Samples with DNA quantification higher than 10 ng are shown in Table 4 (SM). On bronze, only the unsheltered pale green and green patinas allow for successful DNA extraction, while in the sheltered black and dark green sheltered patinas, the DNA is not detectable. On marble, the two patinas (green and white areas) present below the bronze relief of “Pompeo Legnani”, thus affected by the percolation of bronze corrosion products, did not reveal enough environmental DNA to proceed with the biological analysis, so in this statue, DNA was analyzed only in the black area (zone 1 shown in Fig. 1).

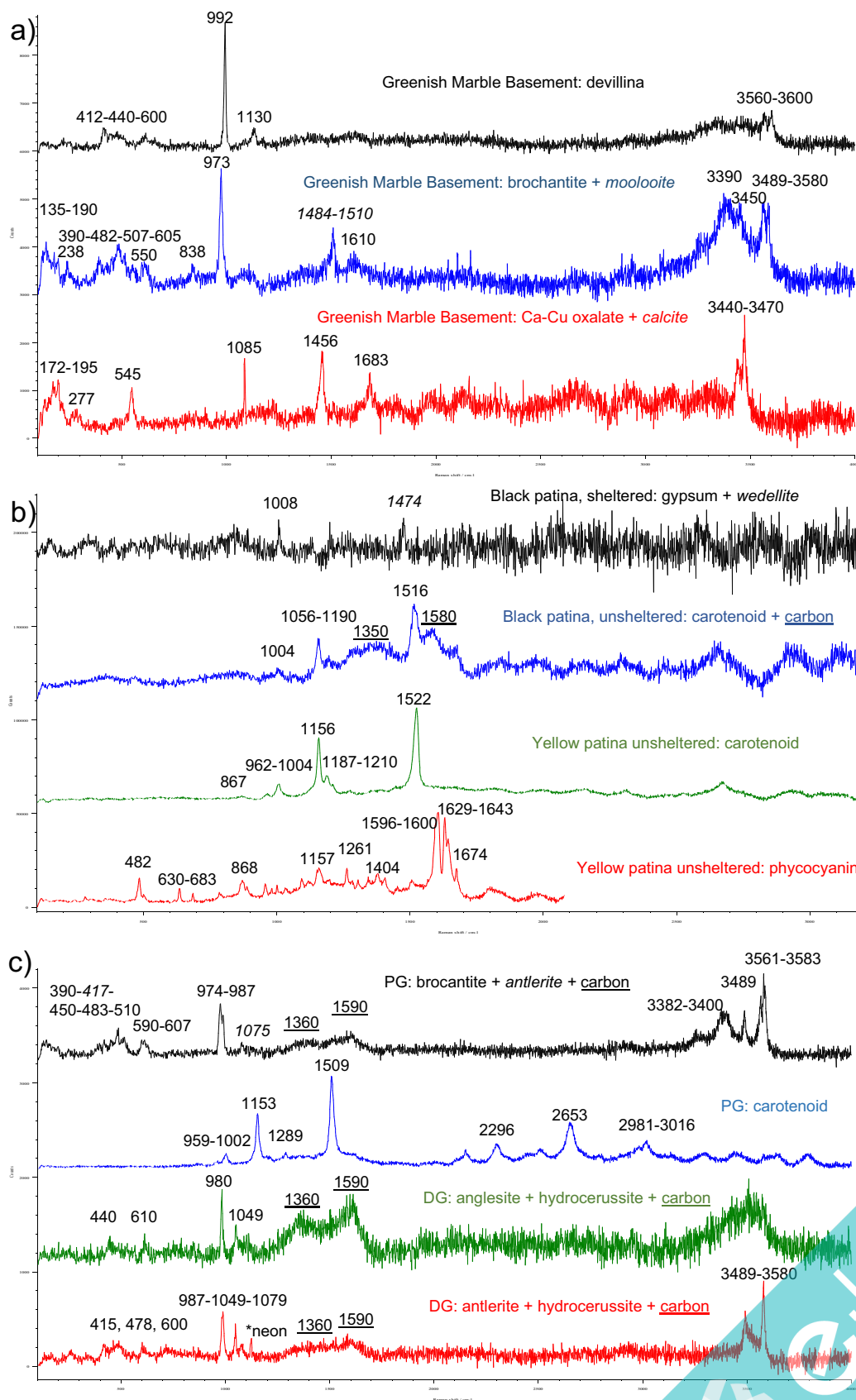


Fig. 3. Raman spectra: (a) greenish marble basement for “Pompeo Legnani” and “Alfredo Oriani” statues; (b) marble statue “Fabbro” (BO): black sheltered, black unsheltered and yellow unsheltered patinas; (c) bronze statue “Trentini Monument” (BO): Pale Green (PG) and Dark green/black (DG).

PROVIDED FOR NON-COMMERCIAL RESEARCH USE AND EDUCATION ONLY. NOT FOR REPRODUCTION, DISTRIBUTION OR COMMERCIAL USE.

Table 3

Mineralogical composition of patinas on bronze and marble (*in bronze patinas, copper oxides are always present, even if not indicated in the table).

Material	Statue's name	Patina colour	Mineralogical composition*
Marble	Pompeo Legnani (BO)	White (<i>unsheltered</i>)	Calcite, quartz and anatase
		Black (<i>unsheltered</i>)	Calcite, carbon and carotenoids
		Green (<i>basement</i>)	Calcite, devilline, and traces of moooloite, antlerite and anatase
	Fabbro (BO)	Black (<i>unsheltered</i>)	Calcite quartz, carotenoids and phycocyanin traces
		Black (<i>sheltered</i>)	Gypsum, carbon and weddellite traces
Bronze	Trentini Monument (BO)	White (<i>unsheltered</i>)	Calcite and carotenoids
		Yellow (<i>unsheltered</i>)	Calcite, carbon, carotenoids and phycocyanins
		Pale green (<i>unsheltered</i>)	Brochantite, antlerite, carbon and carotenoids
		Dark green (<i>sheltered</i>)	Antlerite, anglesite, hydrocerussite carbon and organic substances
	Alfredo Oriani (RA)	Black (<i>sheltered</i>)	Anglesite, hydrocerussite antlerite, carbon and organic substances
		Pale green (<i>unsheltered</i>)	Brochantite, covellite and carbon
		Black (<i>sheltered</i>)	Atacamite, carbon and organic substances and traces of sulfate

4.2.2. Taxonomic composition

Detected contamination was negligible in negative controls, in fact, these samples contained <14 reads. On average $19,453 \pm 18,623$ reads are assigned to bacterial taxa living on marble and 8351 ± 8605 to bronze statues ones.

Bacterial communities living on bronze and marble surfaces show statistically significant differences in terms of composition and structure (Fig. 6, Table 5, SM), indeed the bacterial communities on bronze are characterized by 8 phyla and 30 genera, vs. 9 phyla and 69 genera found on marble statues (Fig. 4a, b).

Bronze patinas show a high abundance of Proteobacteria (90 %) followed by Cyanobacteria (7 %), while the marble patinas show a bacterial community mainly composed of Cyanobacteria (67 %), followed by Proteobacteria (19 %) and Deinococcus-Thermus (10 %).

At the genus level, the bacterial community colonizing the bronze surfaces is mainly composed of *Methylobacterium* (90 %) (Proteobacteria), with the other genera having an abundance of <3 %. Conversely, the bacterial community growing on marble is composed of different genera of Cyanobacteria: *Aliterella* (18 %), *Gloeocapsopsis* (12 %) and *Truepera* (5 %), and Proteobacteria: *Methylobacterium* (12 %), *Sphingomonas* (6 %), *Rubellimicrobium* (3 %) and *Roseomonas* (3 %).

From the characterization carried out on the biofilm on the different patina types: the patina with the highest average number of reads is the Green patina from the “Alfredo Oriani” statue (mean n. reads = $67,560 \pm 89,868$), while the lowest average number of reads is observed on the black sheltered patina belonging to the “Fabbro” (mean n. reads = $48,618 \pm 15,023$). Unsheltered bronze patinas show in common the presence of copper-resistant Proteobacteria, while on the marble ones higher diversity is present.

Specifically, the biofilm living on bronze surfaces shows higher taxa diversity on the “Alfredo Oriani” than on the “Trentini Monument” patinas, especially for pale green ones (Fig. 5a, b). Indeed, they show a presence of Cyanobacteria above 10 % on the “Alfredo Oriani” statue, while these bacteria are almost absent on the pale green patina of the “Trentini Monument” (Fig. 5a, b).

The biofilm occurring on marble surfaces (patinas) shows fewer differences in bacteria composition within the same statue, but some differences occur between the statues; indeed, the two marble statues present two well-differentiated bacterial communities.

Concerning the “Fabbro” statue, the yellow patina shows a bacterial community primarily composed of 85 % Cyanobacteria, 6 % of Deinococcus-Thermus and 6 % of Proteobacteria. Within Cyanobacteria, the most abundant genera are *Aliterella*, *Dapisostemon*, *Gloeocapsopsis* and *Truepera*. The white area shows a following composition: Cyanobacteria 57 %, Proteobacteria 24 % and Deinococcus-Thermus 17 %, the genera most represented are *Anabaena*, *Gelocapsopsis* and *Truepera* (Cyanobacteria), *Deinococcus* (Deinococcus-Thermus) and *Rubellimicrobium* (Proteobacteria). The black area in shadow condition shows the following bacteria composition: Cyanobacteria 85 %, Proteobacteria 7 % and Deinococcus-Thermus 4 %, where *Anabaena*, *Dapisostemon*, *Gelocapsopsis* and *Truepera* (Cyanobacteria) and *Rubellimicrobium* (Proteobacteria) are the most

abundant genera. Concerning the black area (not sheltered) under sunlight conditions, its bacterial community is composed of Cyanobacteria 83 %, Proteobacteria and Deinococcus-Thermus 4 %, with the most abundant genera belonging to Cyanobacteria phylum: *Aliterella*, *Dendronalium*, *Dapisostemon*, *Glocapsopsis*, *Nostoc* and *Truepera*. Therefore, on the whole

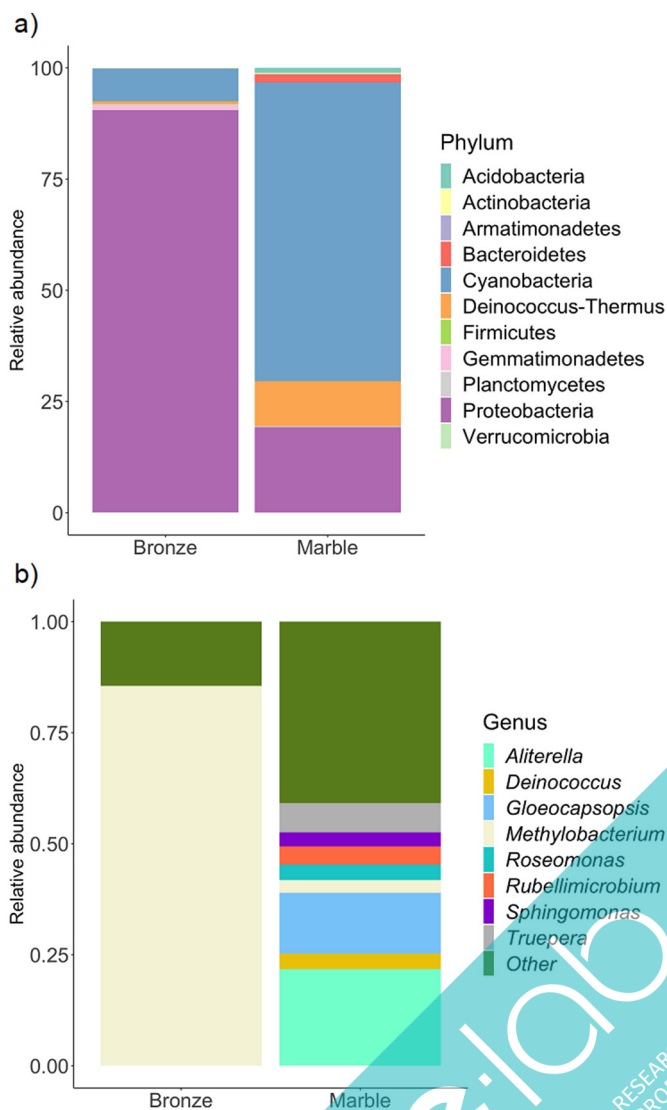


Fig. 4. Bacterial taxonomic profile and relative abundance in Bronze and Marble statues at the phylum level (a) and at the genus level (b). Only abundant taxa included (>0.1 % of total relative abundance). The term “Other” includes all genera with an abundance of <3 %. The histograms are drawn using the R software (Version 4.1.1) ggplot2 package.

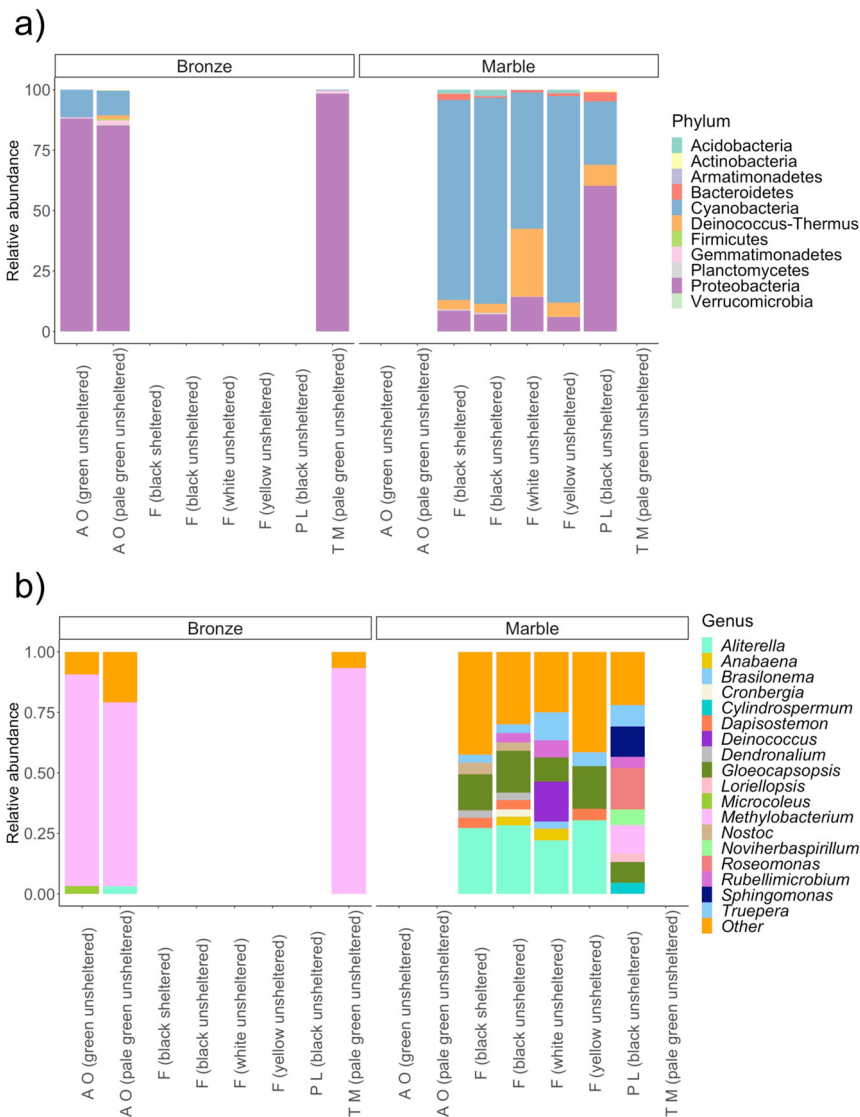


Fig. 5. Bacterial taxonomic profile and abundance of the patina at the phylum level (a) and the genus level (b). Only abundant taxa included (>0.1 % of total relative abundance). The term “Other” includes all genera with an abundance of <3 %. The distribution histogram is drawn based on R software (Version 4.1.1) ggplot2 package. Codes of the analyzed sculptures: A O (Alfredo Oriani), F (Fabbro), P L (Pompeo Legnani), T M (Trentini Monument).

marble “Fabbro” statue, the Cyanobacteria *Aliterella*, *Gloeocapsopsis* and *Truepera* represent the most abundant genera with an abundance >20 %, 10 % and 3 % respectively.

The black area of “Pompeo Legnani” differs from those of the “Fabbro” statue for the greater abundance of Proteobacteria genera and lower presence of Cyanobacteria genera. Indeed, it shows the presence of Proteobacteria for at least 60 %, followed by Cyanobacteria (26 %), Deinococcus-Thermus (9 %) and by Bacteroidetes. At the genus level *Roseomonas*, *Sphingomonas* and *Methylobacterium* (Proteobacteria) represent >17 %, 12 % and 11 %, respectively. Other important genera are *Truepera* (Deinococcus-Thermus) with ~9 %, *Gloeocapsopsis* with ~9 % and *Noviherbaspirillum* (Proteobacteria) with ~6 %.

4.2.3. Alpha diversity

All four diversity indexes show that marble statues host a higher and more significantly diverse bacterial community compared to bronze patinas (Fig. 6, Table 5 SM). No significant differences are observed between the bacterial communities growing on different patina types within the same material, marble or bronze. Indeed, on the bronze patinas, all the diversity indexes show similar results between pale green patina and green patina (Fig. 6, SM) and these values are always lower than those of marble patinas.

Within the marble patinas, those with the highest diversity are the black area of “Pompeo Legnani” and the black area of “Fabbro” in sheltered and shadowed conditions (Fig. 6, SM).

4.2.4. Bacterial community structure

The PERMANOVA and the PCoA reveal significant differences between the bacterial community structure of bronze and marble statues and between patinas within each material (Table 6 SM, Fig. 7). Within Bronze patinas, the bacterial communities are not statistically different both in terms of species richness and abundance ($p = 0.19$, Table 6 SM). Nevertheless, within marble samples, statistically, significant differences are observed between the black area of “Pompeo Legnani” compared to all the other patinas and between the unsheltered black area directly exposed to the sun and white unsheltered patinas (Table 6 SM). Besides, the two replicates belonging to the same patina type always show homogeneity among them.

5. Discussion

For the first time, to our knowledge, we characterize the bacterial communities on bronze and marble artefacts in outdoor conditions and on their

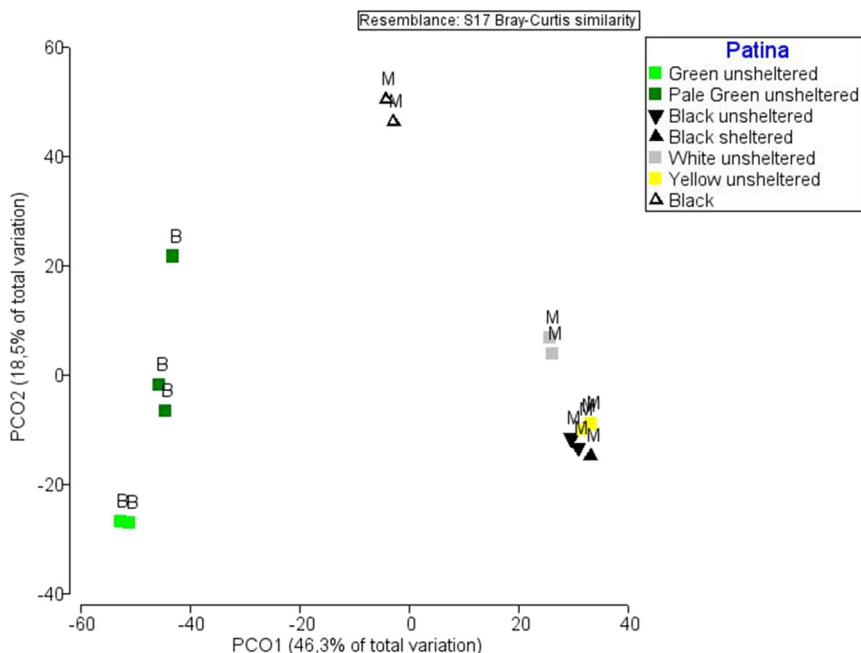


Fig. 7. Principal coordinate analysis plot (PCO) based on a Bray-Curtis distance matrix calculated from the fourth-root transformed OTU abundance data of the bacterial community of the different materials and patinas. B = Bronze, M = Marble. Note that the two uppermost triangles stand for the patinas of the “Pompeo Legnani” statue, the others of marble for the “Fabbro” statue.

associated patinas, using a combination of a non-invasive sampling method and metabarcoding approach.

Differences in DNA concentration and in the bacterial community structure are clearly observed between marble and bronze statues. The lower quantity of eDNA and the lower taxa richness observed in the bronze patinas are likely related to the biocidal effect of copper and lead alloying elements. This was particularly evident for the sheltered black and dark green bronze patinas, where the microbial community characterization was not possible due to very low eDNA. This can be ascribed to the fact that in unsheltered areas, where biological activity was found, the runoff condition leads to the significantly lower biocidal activity of Cu and metal ions, due to: (i) the fast flow of rainwater which reduces the contact time between the surface and the solution enriched in metal ions, thus reducing the activity of Cu ions towards bacteria community; (ii) the solar radiation and higher temperatures that induce faster drying. In sheltered areas and where the surface geometry allows to maintain the surface wet or in stagnant condition for longer times, higher Cu ions concentration is likely attained in the wet period, thus hindering the growth of the biological community. Therefore, free copper ions within the bronze patinas could act as a key factor in the colonization of bacteria and in their diversity, due to their well-known antimicrobial effect (Altimira et al., 2012; Chang et al., 2021a, 2021b; Molteni et al., 2010; Quaranta et al., 2011).

All the marble patinas were characterized by rich and diverse bacterial communities, except for the greenish and white areas in the marble basement of “Pompeo Legnani” where low concentrations of DNA were detected. This gives us further evidence of the detrimental influence of copper and alloying metals leaching from the bronze statue on bacterial communities. Moreover, in both areas, no carotenoids were detected (Table 3) confirming the absence of the phototrophic bacteria community. In these greenish areas, intermediate species between pure Ca-oxalates (weddelite or wewhellite) and Cu-oxalate (moolooite) were detected by Raman analysis. The influence of Cu ions on biological communities can be also inferred by the presence of oxalates in these areas. In fact, the occurrence of oxalates can be ascribed to the reactions of toxic copper ions towards both bacteria, which later died, and/or other living organisms, mostly lichens and fungi (Frank-Kamenetskaya et al., 2021; Joseph, 2021), still not analyzed.

Carotenoids were undetectable also in the white area of the basement, where the low DNA concentration does not allow for the characterization of the bacterial community. The related EDS analyses (Table 2 SM) showed that this area is reached by leached Cu ions; while in the Black area of the “Pompeo Legnani” statue, where both carotenoids and a high abundance of Proteobacteria bacteria were observed, Cu was not detected, even if Proteobacteria are well known to be copper-resistant. Considering that the runoff conditions are the same throughout all the marble basements, this difference between black and green/white areas seems ascribable to the biocidal role of Cu leached by rain and reaching only the green/white areas. Further analyses are necessary to confirm this hypothesis.

Our findings highlight less alpha diversity in bacterial communities growing on bronze statues than on marble statues. This is firstly due to the chemical features, especially the copper cations concentration and release, which detrimentally affect bacterial community structure and growth (Chang et al., 2021a, 2021b), as previously stated. Secondly, the physical characteristics of bronze (i.e., lower porosity and roughness than marble) hinder water retention, which is fundamental for biological growth.

The bacterial community on bronze was characterized by the presence of the only phylum Proteobacteria, with the most abundant genus the facultative methylotroph and oxidase-positive *Methylobacterium*, which also show taxa with characteristic carotene in their membrane (Rizk et al., 2020). The high abundance of this genus in bronze statues could be explained by its high tolerance to copper, as reported by Lejon et al. (2010) and Kunito et al. (2012), who found these microorganisms in soils contaminated by high concentrations of Cu. The genus *Methylobacterium* includes methylotrophic organisms able to metabolize methylated sulfur compounds, such as methanesulfonate CH_3SO_3^- from atmospheric depositions (Sciare et al., 2003), releasing sulfur in the form of HSO_3^- and HSO_4^- (Kelly and Murrell, 1999; Moosvi et al., 2005). This may contribute to further degradation of the bronze substrate, by inducing the growth of sulphates on the patina (brochantite and anglesite), in addition to the environmental contribution from atmospheric SO_2 . Indeed, dimethylsulfide in the atmosphere is expected to increase with climate change (Gabric et al., 2004).

No significant statistical differences were observed in the bacterial communities growing on the different bronze patinas. This may be the

consequence of the general bacteria growth inhibition due to the high amount of copper in the bronze alloy, allowing only the growth of Cu-tolerating genera. Comparing the bronze statues in Ravenna and Bologna, no real biological differences were found, thus no microclimatic influence on bacteria community and structure was found in this work.

Marble patinas are, indeed, characterized by bacterial communities similar to those observed in other CH materials or soil, since bacteria also come from the soil dust resuspension and aerosols (Coelho et al., 2021; Filomena Macedo et al., 2009; Gaylarde et al., 2007; Kunito et al., 2012; Li et al., 2016; Scheerer et al., 2009; Viles and Cutler, 2012).

The most common genera found on marble belong to Cyanobacteria, which generally get energy by photosynthesis and indeed show the presence of photosynthetic pigments (phycobiliproteins, range carotenoid proteins and chlorophyll) (Kay Holt and Krogmann, 1981).

Statistically significant differences in terms of bacterial communities were found between patinas belonging to different marble statues but also between patina types within the same marble statues. Within the “Fabbro” statue, statistical differences occur between the black area directly exposed to the sun (unsheltered) and the white one, while the comparison of “unsheltered black” and “sheltered black” in shadow condition patinas indicates that exposure to sunlight does not induce statistically significant differences. Further research is needed to verify the possible influence of microclimate on microbial composition and structure.

All the “Fabbro” patinas clustered together and were clearly differentiated by the black area belonging to “Pompeo Legnani”. Indeed, all patinas found in the “Fabbro” statue were characterized by a high abundance of Cyanobacteria which are known to be responsible for the discolouration and degradation of the statues (Macedo et al., 2009; Gaylarde et al., 2007; Scheerer et al., 2009), while “Pompeo Legnani” black area shows a more complex and diverse bacterial community with a high abundance of Proteobacteria. This difference can be ascribed to the fact that the “Pompeo Legnani” black area grew on the marble basement close to the greenish stains resulting from copper percolation. Indeed, even if no Cu is detected by EDS (Table 2), this patina shows the highest abundance of Cu and heavy metal-resistant bacteria, such as *Roseomonas*, *Sphingomonas* and *Methylobacterium* (Li et al., 2021; Lopes et al., 2011; Santo et al., 2010; Xie et al., 2012). On the contrary, two genera inhibited by copper, cadmium and lead are not found on this patina: *Aliterella* and especially *Anabaena* (Laube et al., 2011).

Therefore, considering these results, we can state that the composition and structure of the bacteria communities growing on both bronze and green marble patinas subjected to copper percolation are mainly regulated by the Cu and bronze alloying metals biocidal effect, favouring the presence of metal-tolerant genera. In particular, in the case of bronze patina, this selective effect leads to the presence of a very limited number of taxa.

All detected bacterial communities, especially those growing on marble, were characterized by bacteria highly resistant to desiccation, high radiation level, wide and rapid temperature and moisture changes, advocating their capacity to survive under the ongoing climate change conditions (Adhikary et al., 2015; Gaylarde, 2020; Coelho et al., 2021; Crispim and Gaylarde, 2005; Dastager et al., 2008; Gaylarde et al., 2007; Jroundi et al., 2020; Negi and Sarethy, 2019; Urzi, 2004). This is mainly valid for Cyanobacteria, which are expected to increase in abundance and dominate the bacteria communities on cultural heritage artefacts in temperate and Mediterranean Europe, as high temperatures and dry conditions increase (Gladis-Schmacka et al., 2014). Importantly, as Cyanobacteria may produce discolouring and above all structural damages by penetration resulting in boreholes, swelling and shrinking, and thus cracking, disintegration and detachment (Lamenti et al., 2019), their increase may result in increased biodegradation (Scheerer et al., 2009; Viles and Cutler, 2012). Moreover, Proteobacteria seems to be favoured where conditions become drier, as already shown in a study involving a soil microbial community (Castro et al., 2010).

To better understand the differences in the structure of bacterial communities on different patina types, as well as to investigate the specific effects that bacteria communities have on marble and bronze, both

individually and in synergy with outdoor chemical and physical factors, artificial ageing tests in controlled conditions play a key role. They could also give information on possible evolutions of bacterial communities and their effects on the substrate, related to changing environmental conditions. The characterization performed in this study can help the formulation of a bacterial representative community to be included in ageing tests. Here, based on the average relative abundance of bacteria, we propose two communities: for marble patinas, this could be composed mainly of species belonging to the genus *Aliterella*, *Gloeocapsopsis Truepera* and *Rubellimicrobium*; while for bronze surfaces, the proposed bacteria community could be mainly composed of *Methylobacterium*. Finally, in the case of the ageing tests on marble artefacts close to bronze ones, the bacterial community should also include copper-resistant genera such as *Roseomonas*, *Sphingomonas* and *Methylobacterium*.

Runoff or wet-dry (Bernardi et al., 2009; Chiavari et al., 2010) tests coupled with the use of selected bacteria communities are planned to verify the role of the sheltered or unsheltered exposure on their growth.

6. Conclusions

This study performed a characterization of epilithic bacteria communities living on different patinas on marble statues and for the first time also on bronze ones. Strong significant differences in bacteria composition between marble and bronze patinas and a less significant difference between patinas of the same material were found.

Marble surfaces show a high microbial diversity characterized mainly by Cyanobacteria, Proteobacteria and Deinococcus-Thermus. Conversely, on bronze, patinas not exposed to runoff and supposed to stay wet for longer times, like black and dark green patinas, did not contain enough environmental DNA to characterize the communities. Bronze patinas exposed to runoff, like unsheltered pale green patinas, show bacteria communities with low taxa diversity and are dominated by copper-resistant Proteobacteria. The biocidal effect of copper is also confirmed by the analyses on the marble basement of a bronze relief, revealing that in the greenish areas, affected by the percolation of green copper salts, the bacterial community is absent. On the contrary, on the black marble area not directly subject to the percolation of the copper compounds, the bacterial community is present, but the closeness to green Cu-rich areas stimulates the development of copper-resistant bacteria, such as those found in pale green bronze patina (e.g., *Methylobacterium*).

Besides improving the knowledge of bacterial communities living in different areas of bronze and marble sculptures, this study can find applications in cultural heritage conservation since it allows us to propose representative bacterial communities to be included in ageing tests simulating environmental conditions, especially for the Mediterranean and urban areas. The inclusion of currently bacteria communities in material tests simulating tropospheric conditions under climate change will allow to understand the future variation in the bacteria community's structure and in turn the effects of these changes on the material below.

These outcomes are going to be integrated with future biological characterizations of both the overall epilithic community (i.e., fungi and algae) and in different environmental conditions, to combine climate and atmospheric composition changes, likely exacerbating the vulnerability of outdoor materials also via the biological actions.

CRedit authorship contribution statement

Andrea Timoncini: Investigation; Conceptualization; Methodology; Writing - original draft. **Cristina Chiavari:** Conceptualization; Methodology; Investigation; Writing - review & editing; Supervision. **Federica Costantini:** Conceptualization biological characterization analyses; Methodology; Visualization, Review & editing; Supervision Biological Analyses. **Francesco Mugnai:** Investigation biological analyses; Review & editing. **Francesco Paolo Mancuso:** Conceptualization biological Analyses; **Elena Bernardi:** Conceptualization; Methodology, Writing - review & editing. **Carla Martini:** Methodology; Review & Editing. **Francesca Ospitali:**

Investigation Raman analyses; Visualization; Review & Editing. **Enrico Sassoni**: Conceptualisation, Review & Editing.

Data availability

Data will be made available on request.

Declaration of competing interest

The authors declare that they have no known competing financial interests or personal relationships that could have appeared to influence the work reported in this paper.

Acknowledgements

The authors would like to thank the “Museo Civico del Risorgimento di Bologna” (Museum of Italian Unification of the City of Bologna), encompassing the Monumental Cemetery of Bologna, for the opportunity to sample in the Monumental Cemetery. In particular, Dr. Otello Sangiorgi and especially Dr. Roberto Martorelli are gratefully acknowledged for their valuable collaboration.

Appendix A. Supplementary data

Supplementary data to this article can be found online at <https://doi.org/10.1016/j.scitotenv.2022.157804>.

References

- Adamiak, J., Otlewska, A., Tafer, H., Lopandic, K., Gutarowska, B., Sterflinger, K., Piñar, G., 2018a. First evaluation of the microbiome of built cultural heritage by using the ion torrent next generation sequencing platform. *Int. Biodeterior. Biodegrad.* 131, 11–18. <https://doi.org/10.1016/j.ibiod.2017.01.040>.
- Adamiak, J., Otlewska, A., Tafer, H., Lopandic, K., Gutarowska, B., Sterflinger, K., Piñar, G., 2018b. First evaluation of the microbiome of built cultural heritage by using the ion torrent next generation sequencing platform. *Int. Biodeterior. Biodegrad.* 131, 11–18. <https://doi.org/10.1016/j.ibiod.2017.01.040>.
- Adhikary, S.P., Keshari, N., Urzi, C., de Philippis, R., 2015. Cyanobacteria in biofilms on stone temples of Bhubaneswar, eastern India. *Algol. Stud.* 147, 67–93. https://doi.org/10.1127/ALGOL_STUD/2015/0190.
- Albini, M., Chiavari, C., Bernardi, E., Martini, C., Mathys, L., Joseph, E., 2017. Evaluation of the performances of a biological treatment on tin-enriched bronze. *Environ. Sci. Pollut. Res.* 24, 2150–2159. <https://doi.org/10.1007/s11356-016-7361-2/FIGURES/10>.
- Altimira, F., Bravo, G., González, M., Rojas, L.A., Seeger, M., Yaez, C., 2012. Characterization of copper-resistant bacteria and bacterial communities from copper-polluted agricultural soils of central Chile. *BMC Microbiology* 12, 1–12. <https://doi.org/10.1186/1471-2180-12-193/FIGURES/5>.
- Anderson Marti, J., Gorley Ray, N., Robert, Clarke K., 2008. **PERMANOVA + for PRIMER: Guide to Software and Statistical Methods**. PRIMER-E, Plymouth, UK.
- Andreolli, M., Lampis, S., Bernardi, P., Calò, S., Vallini, G., 2020. Bacteria from black crusts on stone monuments can precipitate CaCO₃ allowing the development of a new bio-consolidation protocol for ornamental stone. *Int. Biodeterior. Biodegrad.* 153. <https://doi.org/10.1016/j.ibiod.2020.105031>.
- Bams, V., Dewaele, S., 2007. Staining of white marble. *Mater. Charact.* 58, 1052–1062. <https://doi.org/10.1016/j.MATCHAR.2007.05.004>.
- Baumgartner, L.K., Reid, R.P., Dupraz, C., Decho, A.W., Buckley, D.H., Spear, J.R., Przekop, K.M., Visscher, P.T., 2006. Sulfate reducing bacteria in microbial mats: changing paradigms, new discoveries. *Sediment. Geol.* 185, 131–145. <https://doi.org/10.1016/j.SEDGEO.2005.12.008>.
- Bernard, M.C., Joiret, S., 2009. Understanding corrosion of ancient metals for the conservation of cultural heritage. *Electrochim. Acta* 54, 5199–5205. <https://doi.org/10.1016/j.electacta.2009.01.036>.
- Bernardi, E., Chiavari, C., Lenza, B., Martini, C., Morselli, L., Ospitali, F., Robbiola, L., 2009. The atmospheric corrosion of quaternary bronzes: the leaching action of acid rain. *Corros. Sci.* 51, 159–170. <https://doi.org/10.1016/j.corsci.2008.10.008>.
- Boquet, E., Boronat, A., Ramos-Cormenzana, A., 1973. Production of calcite (calcium carbonate) crystals by soil bacteria is a general phenomenon. *Nature* 5434 (246), 527–529. <https://doi.org/10.1038/246527a0> 1973 246.
- Brimblecombe, P., 2003. The effects of air pollution on the built environment. *Air Pollut. Rev.* 2. <https://doi.org/10.1142/P243>
- Camuffo, D., del Monte, M., Sabbioni, C., Vittori, O., 1982. Wetting, deterioration and visual features of stone surfaces in an urban area. *Atmos. Environ.* 1967 (16), 2253–2259. [https://doi.org/10.1016/0004-6981\(82\)90296-7](https://doi.org/10.1016/0004-6981(82)90296-7).
- Cantisani, E., Cuzman, O.A., Vettori, S., Chelazzi, L., Ciattini, S., Ricci, M., Manganeli Del Fà, R., Chiarantini, L., Garzonio, C.A., 2019. A multi-analytical approach for the study of red stains on heritage marble. *Analyst* 144, 2375–2386. <https://doi.org/10.1039/C8AN02426J>.
- Cao, X., Xu, C., 2006. Synergistic effect of chloride and sulfite ions on the atmospheric corrosion of bronze. *Mater. Corros.* 57, 400–406. <https://doi.org/10.1002/maco.200503936>.
- Castro, H.F., Classen, A.T., Austin, E.E., Norby, R.J., Schadt, C.W., 2010. Soil microbial community responses to multiple experimental climate change drivers. *Appl. Environ. Microbiol.* 76, 999–1007. <https://doi.org/10.1128/AEM.02874-09>.
- Chang, T., Babu, R.P., Zhao, W., Johnson, C.M., Hedström, P., Odnevall, I., Leygraf, C., 2021a. High-resolution microscopical studies of contact killing mechanisms on copper-based surfaces. *ACS Appl. Mater. Interfaces* 13, 49402–49413. <https://doi.org/10.1021/ACSAMI.1C11236>.
- Chang, T., Butina, K., Herting, G., Rajarao, G.K., Richter-Dahlfors, A., Blomberg, E., Odnevall Wallinder, I., Leygraf, C., 2021b. The interplay between atmospheric corrosion and antimicrobial efficiency of Cu and Cu₅Zn₅Al₁Sn during simulated high-touch conditions. *Corros. Sci.* 185, 109433. <https://doi.org/10.1016/j.corsci.2021.109433>.
- Chiavari, C., Rahmouni, K., Takenouti, H., Joiret, S., Vermaut, P., Robbiola, L., 2007. Composition and electrochemical properties of natural patinas of outdoor bronze monuments. *Electrochim. Acta* 52, 7760–7769. <https://doi.org/10.1016/j.electacta.2006.12.053>.
- Chiavari, C., Bernardi, E., Martini, C., Passarini, F., Ospitali, F., Robbiola, L., 2010. The atmospheric corrosion of quaternary bronzes: the action of stagnant rain water. *Corros. Sci.* 52, 3002–3010. <https://doi.org/10.1016/j.corsci.2010.05.013>.
- Chiavari, C., Bernardi, E., Balbo, A., Monticelli, C., Raffo, S., Bignozzi, M.C., Martini, C., 2015. Atmospheric corrosion of fire-gilded bronze: corrosion and corrosion protection during accelerated ageing tests. *Corros. Sci.* 100, 435–447. <https://doi.org/10.1016/j.corsci.2015.08.013>.
- Clarke, K.R., Gorley, R.N., 2015. 85 getting started with PRIMER v7 Plymouth routines in multivariate. *Ecol. Res.* 85.
- Coelho, C., Mesquita, N., Costa, I., Soares, F., Trovão, J., Freitas, H., Portugal, A., Tiago, I., 2021. Bacterial and archaeal structural diversity in several biodeterioration patterns on the limestone walls of the old cathedral of Coimbra. *Microorganisms* 9. <https://doi.org/10.3390/microorganisms9040709>.
- Cole, I.S., Muster, T.H., Paterson, D.A., Furman, S.A., Trinidad, G.S., Wright, N., 2007. Multi-scale modeling of the corrosion of metals under atmospheric corrosion. *Mater. Sci. Forum* 561–565, 2209–2212. <https://doi.org/10.4028/WWW.SCIENTIFIC.NET/MSF.561-565.2209>.
- Crispim, C.A., Gaylarde, C.C., 2005. Cyanobacteria and biodeterioration of cultural heritage: a review. *Microb. Ecol.* <https://doi.org/10.1007/s00248-003-1052-5>.
- Cutler, N., Viles, H., 2010. Eukaryotic microorganisms and stone biodeterioration. *Geomicrobiol. J.* 27, 630–646. <https://doi.org/10.1080/01490451003702933>.
- Dakal, T.C., Cameotra, S.S., 2012. Microbially induced deterioration of architectural heritage: routes and mechanisms involved. *Environ. Sci. Eur.* 24, 1–13. <https://doi.org/10.1186/2190-4715-24-36/FIGURES/1>.
- Daskalakis, M.I., Magoulas, A., Kotoulas, G., Catsikis, I., Bakolas, A., Karageorgis, A.P., Mavridou, A., Doulia, D., Rigas, F., 2013. Pseudomonas, pantoea and cupriavidus isolates induce calcium carbonate precipitation for bioremediation of ornamental stone. *J. Appl. Microbiol.* 115, 409–423. <https://doi.org/10.1111/jam.12234>.
- Dastager, S.G., Lee, J.C., Ju, Y.J., Park, D.J., Kim, C.J., 2008. Rubellimicrobium mesophilum sp. Nov., a mesophilic, pigmented bacterium isolated from soil. *Int. J. Syst. Evol. Microbiol.* 58, 1797–1800. <https://doi.org/10.1099/IJS.0.65590-0/CITE/REFWORKS>.
- Database of Raman Spectroscopy, X-ray Diffraction and Chemistry of Minerals.
- de Oliveira, F.J.R., Lago, D.C.B., Senna, L.F., de Miranda, L.R.M., D'Elia, E., 2009. Study of patina formation on bronze specimens. *Mater. Chem. Phys.* 115, 761–770. <https://doi.org/10.1016/j.matchemphys.2009.02.035>.
- Dias, L., Rosado, T., Candeias, A., Mirão, J., Caldeira, A.T., 2020. Linking ornamental stone discolouration to its biocolonisation state. *Build. Environ.* 180. <https://doi.org/10.1016/j.buildenv.2020.106934>.
- Dupraz, C., Reid, R.P., Braissant, O., Decho, A.W., Norman, R.S., Visscher, P.T., 2009. Processes of carbonate precipitation in modern microbial mats. *Earth Sci. Rev.* 96, 141–162. <https://doi.org/10.1016/j.EARSCIREV.2008.10.005>.
- Erşan, Y.C., de Belie, N., Boon, N., 2015. Microbially induced CaCO₃ precipitation through denitrification: an optimization study in minimal nutrient environment. *Biochem. Eng. J.* 108–118. <https://doi.org/10.1016/j.BEJ.2015.05.006>.
- Filomena Macedo, M., Zélia Miller, A., Saiz-Jimenez, C., Filomena Macedomfmd, M., Lia Dionísio, A., 2009. Biodiversity of cyanobacteria and green algae on monuments in the Mediterranean Basin: an overview. *Microbiology (Reading)*, 3476–3490. <https://doi.org/10.1099/mic.0.032508-0>.
- Frank-Kamenetskaya, O.V., Zelenskaya, M.S., Izatulina, A.R., Vereshchagin, O.S., Vlasov, D.Y., Himelbrant, D.E., Pankin, D.V., 2021. Copper oxalate formation by lichens and fungi. *Sci. Rep.*, 11. <https://doi.org/10.1038/s41598-021-03600-5>.
- Frost, R.L., 2004. Raman spectroscopy of natural oxalates. *Anal. Chim. Acta* 517, 207–214. <https://doi.org/10.1016/j.aca.2004.04.036>.
- Gabric, A.J., Simó, R., Cropp, R.A., Hirst, A.C., Dachs, J., 2004. Modeling estimates of the global emission of dimethylsulfide under enhanced greenhouse conditions. *Glob. Biogeochem. Cycles* 18, 2014. <https://doi.org/10.1029/2003GB002183>.
- Gadd, G.M., Bahri-Esfahani, J., Li, Q., Rhee, Y.J., Wei, Z., Fomina, M., Liang, X., 2014. Oxalate production by fungi: significance in geomycology, biodeterioration and bioremediation. *Fungal Biol. Rev.* <https://doi.org/10.1016/j.fbr.2014.05.001>.
- Gaylarde, C., 2020. Influence of environment on microbial colonization of historic stone buildings with emphasis on cyanobacteria. *Heritage* 3, 1469–1482. <https://doi.org/10.3390/heritage3040081>.
- Gaylarde, C.C., Ortega-Morales, B.O., Bartolo-Pérez, P., 2007. Biogenic black crusts on buildings in unpolluted environments. *Curr. Microbiol.* 54, 162–166. <https://doi.org/10.1007/S00284-006-0432-8/TABLES/2>.
- Ghiara, G., Repetto, L., Piccardo, P., 2019. The effect of Pseudomonas fluorescens on the corrosion morphology of archaeological tin bronze analogues. *JOM* 71, 775–783. <https://doi.org/10.1007/s11837-018-3138-z>.

- Gladis-Schmack, F., Glatzel, S., Karsten, U., Böttcher, H., Schumann, R., 2014. Influence of local climate and climate change on aerorespiratory phototrophic biofilms. *Biofouling* 30, 401–414. <https://doi.org/10.1080/08927014.2013.878334>.
- Gómez-Bolea, A., Llop, E., Ariño, X., Saiz-Jimenez, C., Bonazza, A., Messina, P., Sabbioni, C., 2012. Mapping the impact of climate change on biomass accumulation on stone. *J. Cult. Herit.* 13, 254–258. <https://doi.org/10.1016/j.culher.2011.10.003>.
- Graedel, T.E., Nassau, K., Franey, J.P., 1987. Copper patinas formed in the atmosphere-Introduction. *Corros. Sci.* 27, 639–657. [https://doi.org/10.1016/0010-938X\(87\)90047-3](https://doi.org/10.1016/0010-938X(87)90047-3).
- Grottoli, A., Beccacoli, M., Zoppis, E., Fratini, R.S., Schifano, E., Santarelli, M.L., Uccelletti, D., Reverberi, M., 2020. Nanopore sequencing and bioinformatics for rapidly identifying cultural heritage spoilage microorganisms. *Front. Mater.* 7. <https://doi.org/10.3389/fmats.2020.00014>.
- Guillitte, O., 1995. Bioreceptivity: a new concept for building ecology studies. *Sci. Total Environ.* 167, 215–220. [https://doi.org/10.1016/0048-9697\(95\)04582-L](https://doi.org/10.1016/0048-9697(95)04582-L).
- Hammes, F., Verstraete, W., 2002. Key roles of pH and calcium metabolism in microbial carbonate precipitation. *Rev. Environ. Sci. Biotechnol.* 1, 3–7. <https://doi.org/10.1023/A:1015135629155> 2002 1:1.
- Hammes, F., Boon, N., de Villiers, J., Verstraete, W., Siciliano, S.D., 2003. Strain-specific ureolytic microbial calcium carbonate precipitation. *Appl. Environ. Microbiol.* 69, 4901. <https://doi.org/10.1128/AEM.69.8.4901-4909.2003>.
- Hayez, V., Guillaume, J., Hubin, A., Terryn, H., 2004. Micro-Raman spectroscopy for the study of corrosion products on copper alloys: setting up of a reference database and studying works of art. *J. Raman Spectrosc.* 35, 732–738. <https://doi.org/10.1002/JRS.1194>.
- Joseph, E., 2021. Biopassivation method for the preservation of copper and bronze artefacts. *Front. Mater.* 7. <https://doi.org/10.3389/FMATS.2020.613169>.
- Joseph, E., Cario, S., Simon, A., Wörle, M., Mazzeo, R., Junier, P., Job, D., 2012. Protection of metal artifacts with the formation of metal-oxalates complexes by *Beauveria bassiana*. *Front. Microbiol.* 2, 270. <https://doi.org/10.3389/FMICB.2011.00270/BIBTEX>.
- Jroundi, F., Elert, K., Ruiz-Agudo, E., Gonzalez-Muñoz, M.T., Rodriguez-Navarro, C., 2020. Bacterial diversity evolution in Maya painting and stone following a bio-conservation treatment. *Front. Microbiol.* 11. <https://doi.org/10.3389/FMICB.2020.599144/FULL>.
- Kay Holt, T., Krogmann, D.W., 1981. A carotenoid-protein from cyanobacteria. *Biochim. Biophys. Acta Bioenerg.* 637, 408–414. [https://doi.org/10.1016/0005-2728\(81\)90045-1](https://doi.org/10.1016/0005-2728(81)90045-1).
- Kelly, D.P., Murrell, J.C., 1999. Microbial metabolism of methanesulfonic acid. *Arch. Microbiol.* 172 (6), 341–348. <https://doi.org/10.1007/S002030050770>.
- Kemmling, A., Kämper, M., Flies, C., Schieweck, O., Hoppert, M., 2004. Biofilms and extracellular matrices on geomaterials. *Environ. Geol.* 46, 429–435. <https://doi.org/10.1007/S00254-004-1044-X>.
- Kip, N., van Veen, J.A., 2015. The dual role of microbes in corrosion. *ISME J.* <https://doi.org/10.1038/ismej.2014.169>.
- Kong, D.C., Dong, C.F., Fang, Y.H., Xiao, K., Guo, C.Y., He, G., Li, X.G., 2016. Long-term corrosion of copper in hot and dry atmosphere in Turpan, China. *J. Mater. Eng. Perform.* 7, 2977–2984. <https://doi.org/10.1007/S11665-016-2114-4>.
- Kunito, T., Nagaoka, K., Tada, N., Saeki, K., Senoo, K., Oyaizu, H., Matsumoto, S., 2012. Soil Science and Plant Nutrition Characterization of Cu-resistant Bacterial Communities in Cu-contaminated Soils. <https://doi.org/10.1080/00380768.1997.10414795>.
- Lamenti, G., Tomaselli, L., Tian, P., 2019. Cyanobacteria and biodeterioration of monumental stones. *Molecular Biology and Cultural Heritage*. Routledge, pp. 73–78. <https://doi.org/10.1201/9780203746578-9>.
- Laube, V.M., McKenzie, C.N., Kushner, D.J., 2011. Strategies of Response to Copper, Cadmium, and Lead by a Blue-green and a Green Alga. 26, pp. 1300–1311. <https://doi.org/10.1139/M80-217>.
- Lejon, D.P.H., Pascault, N., Ranjard, L., 2010. Differential copper impact on density, diversity and resistance of adapted culturable bacterial populations according to soil organic status. *Eur. J. Soil Biol.* 46, 168–174. <https://doi.org/10.1016/J.EJSOBI.2009.12.002>.
- Li, Q., Zhang, B., He, Z., Yang, X., 2016. Distribution and diversity of bacteria and fungi colonization in stone monuments analyzed by high-throughput sequencing. *PLoS ONE* 11. <https://doi.org/10.1371/journal.pone.0163287>.
- Li, F., Huang, Y., Hu, W., Li, Z., Wang, Q., Huang, S., Jiang, F., Pan, X., 2021. *Roseomonas coralli* sp. nov., a heavy metal resistant bacterium isolated from coral. *Int. J. Syst. Evol. Microbiol.* 71, 1–7. <https://doi.org/10.1099/IJSEM.0.004624/CITE/REFWORKS>.
- Lipfert, F.W., 1989. Atmospheric damage to calcareous stones: comparison and reconciliation of recent experimental findings. *Atmos. Environ.* 23 (2), 415–429.
- Liu, B., Wang, D.W., Guo, H., Ling, Z.H., Cheung, K., 2015. Metallic corrosion in the polluted urban atmosphere of Hong Kong. *Environ. Monit. Assess.* 187. <https://doi.org/10.1007/s10661-014-4112-z>.
- Lopes, A., Santo, C.E., Grass, G., Chung, A.P., Morais, P., v., 2011. *Roseomonas pecuniae* sp. Nov., isolated from the surface of a copper-alloy coin. *Int. J. Syst. Evol. Microbiol.* 61, 610–615. <https://doi.org/10.1099/IJSEM.0.020966-0/CITE/REFWORKS>.
- Macedo, M.F., Miller, A.Z., Dionísio, A., Saiz-Jimenez, C., 2009. Biodiversity of cyanobacteria and green algae on monuments in the Mediterranean Basin: an overview. *Microbiology (N Y)* <https://doi.org/10.1099/mic.0.032508-0>.
- Magi, A., Semeraro, R., Mingrino, A., Giusti, B., D'Aurizio, R., 2017. Nanopore sequencing data analysis: state of the art, applications and challenges. *Brief. Bioinform.* 19, 1256–1272. <https://doi.org/10.1093/bib/bbx062>.
- Margalef, R., 1958. Information theory in biology. *General Systems Yearbook* 3, pp. 36–71.
- Martens, W., Frost, R.L., Klopogge, J.T., Williams, P.A., 2003. Raman spectroscopic study of the basic copper sulphates - implications for copper corrosion and “bronze disease”. *J. Raman Spectrosc.* 34, 145–151. <https://doi.org/10.1002/jrs.969>.
- McMurdie, P.J., Holmes, S., 2013. Phyloseq: an R package for reproducible interactive analysis and graphics of microbiome census data. *PLOS ONE* 8, e61217. <https://doi.org/10.1371/JOURNAL.PONE.0061217>.
- Molteni, C., Abicht, H.K., Solioz, M., 2010. Killing of bacteria by copper surfaces involves dissolved copper. *Appl. Environ. Microbiol.* 76, 4099–4101. <https://doi.org/10.1128/AEM.00424-10>.
- Monks, P.S., Granier, C., Fuzzi, S., Stohl, A., Williams, M.L., Akimoto, H., Amann, M., Baklanov, A., Baltensperger, U., Bey, I., Blake, N., Blake, R.S., Carslaw, K., Cooper, O.R., Dentener, F., Fowler, D., Fragkou, E., Frost, G.J., Generoso, S., Ginoux, P., Grew, V., Guenther, A., Hansson, H.C., Henne, S., Hjorth, J., Hofzumahaus, A., Huntrieser, H., Isaksen, I.S.A., Jenkin, M.E., Kaiser, J., Kanakidou, M., Klimont, Z., Kulmala, M., Laj, P., Lawrence, M.G., Lee, J.D., Liousse, C., Maione, M., McFiggans, G., Metzger, A., Mieville, A., Moussiopoulos, N., Orlando, J.J., O'Dowd, C.D., Palmer, P.I., Parrish, D.D., Petzold, A., Platt, U., Pöschl, U., Prévôt, A.S.H., Reekes, C.E., Reimann, S., Rudich, Y., Sellegri, K., Steinbrecher, R., Simpson, D., ten Brink, H., Theloke, J., van der Werf, G.R., Vautard, R., Vestreng, V., Vlachokostas, C., von Glasow, R., 2009. Atmospheric composition change - global and regional air quality. *Atmos. Environ.* <https://doi.org/10.1016/j.atmosenv.2009.08.021>.
- Monte, M., 2003. Oxalate film formation on marble specimens caused by fungus. *J. Cult. Herit.* 4, 255–258. [https://doi.org/10.1016/S1296-2074\(03\)00051-7](https://doi.org/10.1016/S1296-2074(03)00051-7).
- Moosvi, S.A., McDonald, I.R., Pearce, D.A., Kelly, D.P., Wood, A.P., et al., 2005. Molecular detection and isolation from Antarctica of methylotrophic bacteria able to grow with methylated sulfur compounds. *Syst. Appl. Microbiol.* 28 (6), 541–554. <https://doi.org/10.1016/J.SYAPM.2005.03.002>.
- Muros, V., Scott, D.A., 2018. The occurrence of brochantite on archaeological bronzes: a case study from Lofkënd, Albania. *Stud. Conserv.* 63, 113–125. <https://doi.org/10.1080/00393630.2016.1264179>.
- Nassau, K., Gallagher, P.K., Miller, A.E., Graedel, T.E., 1987. The characterization of patina components by X-ray diffraction and evolved gas analysis. *Corros. Sci.* 27, 669–684. [https://doi.org/10.1016/0010-938X\(87\)90049-7](https://doi.org/10.1016/0010-938X(87)90049-7).
- Negi, A., Sarethy, I.P., 2019. Microbial biodeterioration of cultural heritage: events, colonization, and analyses. *Microb. Ecol.* 78, 1014–1029. <https://doi.org/10.1007/S00248-019-01366-Y/TABLES/1>.
- Nygaard, A.B., Tunsjø, H.S., Meisal, R., Charnock, C., 2020. A preliminary study on the potential of nanopore MinION and illumina MiSeq 16S rRNA gene sequencing to characterize building-dust microbiomes. *Sci. Rep.* 10, 3209. <https://doi.org/10.1038/s41598-020-59771-0>.
- Ortega-Morales, O., Montero-Muñoz, J.L., Baptista Neto, J.A., Beech, I.B., Sunner, J., Gaylarde, C., 2019. Deterioration and microbial colonization of cultural heritage stone buildings in polluted and unpolluted tropical and subtropical climates: a meta-analysis. *Int. Biodeterior. Biodegrad.* 143. <https://doi.org/10.1016/j.ibiod.2019.104734>.
- Ortega-Villamagua, E., Gudiño-Gomezjurado, M., Palma-Cando, A., 2020. Microbiologically induced carbonate precipitation in the restoration and conservation of cultural heritage materials. *Molecules* <https://doi.org/10.3390/molecules25235499>.
- Pachauri, R.K., Allen, M.R., Barros, V.R., Broome, J., Cramer, W., Christ, R., Church, J.A., Clarke, L., Dahe, Q., Dasgupta, P., Dubash, N.K., Edenhofer, O., Elgizouli, I., Field, C.B., Forster, P., Friedlingstein, P., Fuglestedt, J., Gomez-Echeverri, L., Hallegatte, S., Hegger, G., Howden, M., Jiang, K., Jimenez Cisneros, B., Kattsov, V., Lee, H., Mach, K.J., Marotzke, J., Mastrandrea, M.D., Meyer, L., Minx, J., Mulugetta, Y., O'Brien, K., Oppenheimer, M., Pereira, J.J., Pichs-Madruga, R., Plattner, G.-K., Pörtner, H.-O., Power, S.B., Preston, B., Ravindranath, N.H., Reisinger, A., Riahii, K., Rusticucci, M., Scholes, R., Seyboth, K., Sokona, Y., Stavins, R., Stocker, T.F., Tschakert, P., van Vuuren, D., van Ypersele, J.-P., 2014. Climate Change 2014: Synthesis Report. Contribution of Working Groups I, II and III to the Fifth Assessment Report of the Intergovernmental Panel on Climate Change. EPIC3Geneva, Switzerland, IPCC. ISBN: 978-92-9169-143-2, p. 151 151 p.
- Pavlovic, J., Cavalieri, D., Mastromei, G., Pangallo, D., Perito, B., Marvasi, M., 2021. MinION technology for microbiome sequencing applications for the conservation of cultural heritage. *Microbiol. Res.* <https://doi.org/10.1016/j.micres.2021.126727>.
- Perez-Rodriguez, J.L., Duran, A., Centeno, M.A., Martinez-Blanes, J.M., Robador, M.D., 2011. Thermal analysis of monument patina containing hydrated calcium oxalates. *Thermochim. Acta* 512, 5–12. <https://doi.org/10.1016/J.TCA.2010.08.015>.
- Piccardo, P., Bongiorno, V., Campodonico, S., 2013. Artistic patinas on ancient bronze statues. Corrosion and Conservation of Cultural Heritage Metallic Artefacts. 193–212. <https://doi.org/10.1533/9781782421573.3.193>.
- Picciochi, R., Ramos, A.C., Mendonça, M.H., Fonseca, I.T.E., 2004. Influence of the environment on the atmospheric corrosion of bronze. *J. Appl. Electrochem.* 34 (10), 989–995. <https://doi.org/10.1023/B:JACH.000042667.84920.E2> 151 p.
- Pielou, E.C., 1966. The measurement of diversity in different types of biological collections. *J. Theor. Biol.* 13, 131–144.
- Piñar, G., Poyntner, C., Tafer, H., Sterflinger, K., 2019. A time travel story: metagenomic analyses decipher the unknown geographical shift and the storage history of possibly smuggled antique marble statues. *Ann. Microbiol.* 69, 1001–1021. <https://doi.org/10.1007/S13213-019-1446-3/FIGURES/6>.
- Piñar, G., Poyntner, C., Lopandic, K., Tafer, H., Sterflinger, K., 2020a. Rapid diagnosis of biological colonization in cultural artefacts using the MinION nanopore sequencing technology. *Int. Biodeterior. Biodegrad.* 148. <https://doi.org/10.1016/j.ibiod.2020.104908>.
- Piñar, G., Sclocchi, M.C., Pinzari, F., Colaizzi, P., Graf, A., Sebastiani, M.L., Sterflinger, K., 2020b. The microbiome of Leonardo da Vinci's drawings: a bio-archive of their history. *Front. Microbiol.* 11, 2889. <https://doi.org/10.3389/FMICB.2020.593401/BIBTEX>.
- Prieto, B., Silva, B., Lantes, O., 2004. Biofilm quantification on stone surfaces: comparison of various methods. *Sci. Total Environ.* 333, 1–7. <https://doi.org/10.1016/j.scitotenv.2004.05.003>.
- Prieto, B., Vázquez-Nion, D., Fuentes, E., Durán-Román, A.G., 2020. Response of subaerial biofilms growing on stone-built cultural heritage to changing water regime and CO₂ conditions. *Int. Biodeterior. Biodegrad.* 148. <https://doi.org/10.1016/j.ibiod.2019.104882>.
- Pyzik, A., Ciuchcinski, K., Dziurzynski, M., Dzięwit, L., 2021. The bad and the good-microorganisms in cultural heritage environments-an update on biodeterioration and biotreatment approaches. *Materials* <https://doi.org/10.3390/ma14010177>.

- Quaranta, D., Krans, T., Santo, C.E., Elowsky, C.G., Domaille, D.W., Chang, C.J., Grass, G., 2011. Mechanisms of contact-mediated killing of yeast cells on dry metallic copper surfaces. *Appl. Environ. Microbiol.* 77, 416–426. <https://doi.org/10.1128/AEM.01704-10>.
- R Core Team, 2021. R: A Language and Environment for Statistical Computing. R Foundation for Statistical Computing, Vienna, Austria. <https://www.R-project.org/>.
- Ramirez, M., Hernandez-Marine, M., Novelo, E., Roldan, M., 2010. Cyanobacteria-containing biofilms from a mayan monument in Palenque, Mexico. *Biofouling* 26, 399–409. <https://doi.org/10.1080/08927011003660404>.
- Rizk, S., Henke, P., Santana-Molina, C., Martens, G., Gnädig, M., Devos, D.P., Neumann-Schaal, M., Saenz, J.P., 2020. Functional diversity of isoprenoidal lipids in *Methylobacterium extorquens* PA1. *bioRxiv* <https://doi.org/10.1101/2020.12.21.423902>.
- Rodriguez-Navarro, C., Rodriguez-Gallego, M., Chekroun, K.Ben, Gonzalez-Muñoz, M.T., 2003. Conservation of ornamental stone by *Myxococcus xanthus*-induced carbonate biomineralization. *Appl. Environ. Microbiol.* 69, 2182. <https://doi.org/10.1128/AEM.69.4.2182-2193.2003>.
- Sabbioni, C., Cassar, M., Brimblecombe, P., 2010. The Atlas of Climate Change Impact on European Cultural Heritage. Anthem Press, London. <https://doi.org/10.2777/11959>.
- Salinas-Nolasco, M.F., Méndez-Vivar, J., Lara, V.H., Bosch, P., 2004. Passivation of the calcite surface with malonate ion. *J. Colloid Interface Sci.* 274, 16–24. <https://doi.org/10.1016/J.JCIS.2003.10.027>.
- Samie, F., Tidblad, J., Kucera, V., Leygraf, C., 2007. Atmospheric corrosion effects of HNO₃-comparison of laboratory-exposed copper, zinc and carbon steel. *Atmos. Environ.* 41, 4888–4896. <https://doi.org/10.1016/j.atmosenv.2007.02.007>.
- Sand, W., Jozsa, P.-G., Mansch, R., 2003. Weathering. *Microbiol. Encyclopedia of Environmental Microbiology*. <https://doi.org/10.1002/0471263397.ENV286>.
- Sanmartín, P., DeAraujo, A., Vasanthakumar, A., Mitchell, R., 2015. Feasibility study involving the search for natural strains of microorganisms capable of degrading graffiti from heritage materials. *Int. Biodeterior. Biodegrad.* 103, 186–190. <https://doi.org/10.1016/J.IBID.2015.05.010>.
- Santo, C.E., Morais, P.V., Grass, G., 2010. Isolation and characterization of bacteria resistant to metallic copper surfaces. *Appl. Environ. Microbiol.* 76, 1341–1348. https://doi.org/10.1128/AEM.01952-09/SUPPL_FILE/SUPPLEMENTAL_MATERIAL_GRASS_COPPER.DOC.
- Santos, A., van Aerle, R., Barrientos, L., Martínez-Urtaza, J., 2020. Computational methods for 16S metabarcoding studies using nanopore sequencing data. *Comput. Struct. Biotechnol. J.* <https://doi.org/10.1016/j.csbj.2020.01.005>.
- Scheerer, S., Ortega-Morales, O., Gaylarde, C., 2009. Chapter 5 microbial deterioration of stone monuments—an updated overview. *Adv. Appl. Microbiol.* [https://doi.org/10.1016/S0065-2164\(08\)00805-8](https://doi.org/10.1016/S0065-2164(08)00805-8).
- Schröer, L., Boon, N., de Kock, T., Cnudde, V., 2021. The capabilities of bacteria and archaea to alter natural building stones—a review. *Int. Biodeterior. Biodegrad.* 165, 964–8305. <https://doi.org/10.1016/j.ibid.2021.105329>.
- Schröer, L., de Kock, T., Godts, S., Boon, N., Cnudde, V., 2022. The effects of cyanobacterial biofilms on water transport and retention of natural building stones. *Earth Surf. Process. Landf.* <https://doi.org/10.1002/ESP.5355>.
- Schulz, H., Baranska, M., Baranski, R., 2005. Potential of NIR-FT-Raman spectroscopy in natural carotenoid analysis. *Biopolymers* 77, 212–221. <https://doi.org/10.1002/BIP.20215>.
- Sciare, J., Bardouki, H., Moulin, C., Mihalopoulos, N., et al., 2003. Atmospheric Chemistry and Physics Aerosol sources and their contribution to the chemical composition of aerosols in the Eastern Mediterranean Sea during summertime. *Atmos. Chem. Phys.* 3 (1), 291–302. <https://doi.org/10.5194/acp-3-291-2003>.
- Seinfeld, J.H., Pandis, S.N., 2016. *Atmospheric Chemistry and Physics: From Air Pollution to Climate Change*. Third edition. 1152. Wiley & Sons, Inc, Hoboken, New Jersey USA New Jersey USA.
- Solomon, S., Intergovernmental Panel on Climate Change, Intergovernmental Panel on Climate Change. Working Group I, 2007. *Climate Change 2007: The Physical Science Basis: Contribution of Working Group I to the Fourth Assessment Report of the Intergovernmental Panel on Climate Change*. Cambridge University Press.
- Spezzano, P., 2021. Mapping the susceptibility of UNESCO world cultural heritage sites in Europe to ambient (outdoor) air pollution. *Sci. Total Environ.* 754. <https://doi.org/10.1016/j.scitotenv.2020.142345>.
- Stocks-Fischer, S., Galinat, J.K., Bang, S.S., 1999. Microbiological precipitation of CaCO₃. *Soil Biol. Biochem.* 31, 1563–1571. [https://doi.org/10.1016/S0038-0717\(99\)00082-6](https://doi.org/10.1016/S0038-0717(99)00082-6).
- Szalontai, B., Gombos, Z., Csizmadia, V., Bagyinka, C., Lutz, M., 1994. Structure and interactions of phycocyanobilin chromophores in phycocyanin and allophycocyanin from an analysis of their resonance Raman spectra. *Biochemistry* 33, 11823–11832. <https://doi.org/10.1021/BIO0205A019>.
- Tidblad, J., Hicks, K., Kuylenstierna, J., Pradhan, B.B., Dangol, P., Mylvakanam, I., Feresu, S.B., Lungu, C., 2016. Atmospheric corrosion effects of air pollution on materials and cultural property in Kathmandu, Nepal. *Mater. Corros.* 67, 170–175. <https://doi.org/10.1002/MACO.201408043>.
- Toreno, G., Isola, D., Meloni, P., Carcangiu, G., Selbmann, L., Onofri, S., Caneva, G., Zucconi, L., 2018. Biological colonization on stone monuments: a new low impact cleaning method. *J. Cult. Herit.* 30, 100–109. <https://doi.org/10.1016/j.culher.2017.09.004>.
- Tourney, J., Ngwenya, B.T., 2014. The role of bacterial extracellular polymeric substances in geomicrobiology. *Chem. Geol.* 386, 115–132. <https://doi.org/10.1016/J.CHEMGEO.2014.08.011>.
- Urzi, C., 2004. Microbial deterioration of rocks and marble monuments of the Mediterranean basin: a review. *Corros. Rev.* 22, 441–457. <https://doi.org/10.1515/CORRREV.2004.22.5-6.441/MACHINEREADABLECITATION/RIS>.
- Vergès-Belmin, V., Cartwright, Tamara Anson, Bourguignon, Elsa, Bromblet, Philippe, Cassar, Jo Ann, Charola, A.Elena, Witte, Eddy De, Delgado-Rodríguez, Jose, Fassina, Vasco, Fitzne, Bernd, Fortier, Laurent, Franzen, Christoph, de Miguel, José-Maria Garcia, Hyslop, Ewan, Kwiatkowski, Daniel, Krumbain, Wolfgang E., Lefèvre, Roger-Alexandre, Klingspor-Rotstein, Marie, Maxwell, Ingvál, McMillan, Andrew, Michoinova, Dagmar, Nishiura, Tadateru, Normandin, Kyle, Queisser, Andreas, Pallot-Frossard, Isabelle, Poshyanandana, Vasu, Scherer, George W., Simon, Stefan, Snethlage, Rolf, Tourneur, Francis, Vallet, Jean-Marc, Hees, Rob Van, Varti-Matarangas, Myrsini, Vergès-Belmin, Véronique, Warscheid, Tomas, Winterhalter, Kati, Young, David, 2008. *ICOMOS-ISCS: Illustrated Glossary on Stone Deterioration Patterns Glossaire illustré sur les formes d'altération de la pierre MONUMENTS AND SITES MONUMENTS ET SITES XV*.
- Vidal, F., Vicente, R., Mendes Silva, J., 2019. Review of environmental and air pollution impacts on built heritage: 10 questions on corrosion and soiling effects for urban intervention. *J. Cult. Herit.* <https://doi.org/10.1016/j.culher.2018.11.006>.
- Videla, H.A., Herrera, L.K., 2009. Understanding microbial inhibition of corrosion. A comprehensive overview. *Int. Biodeterior. Biodegrad.* 63, 896–900. <https://doi.org/10.1016/j.ibid.2009.02.002>.
- Viles, H.A., Cutler, N.A., 2012. Global environmental change and the biology of heritage structures. *Glob. Chang. Biol.* 18, 2406–2418. <https://doi.org/10.1111/J.1365-2486.2012.02713.X>.
- von Schneidmesser, E., Monks, P.S., Allan, J.D., Bruhwiler, L., Forster, P., Fowler, D., Lauer, A., Morgan, W.T., Paasonen, P., Righi, M., Sindelarova, K., Sutton, M.A., 2015. Chemistry and the linkages between air quality and climate change. *Chem. Rev.* <https://doi.org/10.1021/acs.chemrev.5b00089>.
- Wakefield, R.D., Jones, M.S., 1998. An introduction to stone colonizing micro-organisms and biodeterioration of building stone. *Q. J. Eng. Geol. Hydrogeol.* 31, 301–313. <https://doi.org/10.1144/GSL.QJEG.1998.031.P4.03>.
- Warscheid, T., Braams, J., 2000. Biodeterioration of stone: a review. *Int. Biodeterior.* 46 (4), 343–368. [https://doi.org/10.1016/S0964-8305\(00\)00109-8](https://doi.org/10.1016/S0964-8305(00)00109-8).
- Watt, J., Tidblad, J., Hamilton, R., Kucera, V., et al., 2009. *The Effects of Air Pollution on Cultural Heritage*. Springer, New York, NY, pp. 1–306.
- Xie, X., Fu, J., Wang, H., Liu, J., 2012. Heavy metal resistance by two bacteria strains isolated from a copper mine tailing in China. *Afr. J. Biotechnol.* 9, 4056–4066. <https://doi.org/10.4314/ajb.v9i26>.
- Zanardini, E., Abbruscato, P., Ghedini, N., Realini, M., Sorlini, C., 2000. Influence of atmospheric pollutants on the biodeterioration of stone. *Int. Biodeterior. Biodegrad.* 45, 35–42. [https://doi.org/10.1016/S0964-8305\(00\)00043-3](https://doi.org/10.1016/S0964-8305(00)00043-3).